Food Frontiers

FOOD FRONTIERS Open Access

RESEARCH ARTICLE OPEN ACCESS

Anthocyanin Extracts From 11 Superfruits Mitigate Oxidative Stress and Inflammatory Damage in HK-2 Cells Induced by Cadmium Exposure

Jiaojiao Liang[1] | Yunyi Chen[1] | Manxi Wu[1] | Jiebiao Chen[1] | Cui Sun[2] | Jinping Cao[1,2] | Yue Wang[1,3] | Chongde Sun[1,2]

[1]Laboratory of Fruit Quality Biology/The State Agriculture Ministry Laboratory of Horticultural Plant Growth, Development and Quality Improvement, Fruit Science Institute, College of Agriculture and Biotechnology, Zhejiang University, Hangzhou, China | [2]Hainan Institute of Zhejiang University, Sanya, Hainan, People's Republic of China | [3]Center for Balance Architecture, Zhejiang University, Hangzhou, China

Correspondence: Chongde Sun (adesun2006@zju.edu.cn)

Received: 9 January 2025 | **Revised:** 24 February 2025 | **Accepted:** 22 March 2025

Funding: This article was supported by the National Natural Science Foundation of China (32101932) and the Zhejiang Province Natural Science Foundation Joint Fund Project (LHZSD24C150001).

Keywords: anthocyanin | cadmium | oxidative stress | superfruits

ABSTRACT

Cadmium (Cd) pollution has emerged as an escalating threat to human health, with its induced kidney toxicity being closely linked to oxidative stress and inflammation. In this study, we extracted and analyzed primary anthocyanins from 11 superfruits using UPLC-Triple-TOF/MS and evaluated their antioxidant capacity through DPPH, ABTS, FRAP, and ORAC assays. By employing a Cd-exposed Human Kidney-2 (HK-2) cells injury model, we investigated the protective effects of superfruit anthocyanin extracts. The results demonstrated that these extracts enhanced HK-2 cell viability, increased T-SOD and GSH levels, and reduced ROS, MDA, and NO. Furthermore, they significantly regulated oxidative stress and inflammation-related genes and proteins. Moreover, we elucidated the mechanisms by which these anthocyanins mitigate Cd-induced cellular damage via classical oxidative and inflammatory pathways. These findings highlight the potential of specific anthocyanin-rich fruits in reducing Cd-related health risks and suggest practical applications for their bioactive properties in promoting human health.

1 | Introduction

Unlike commonly cultivated bulk fruits, certain fruits that are grown on a small scale under specific climatic or regional conditions exhibit unique shapes, colors, or flavors. These fruits often accumulate higher levels of bioactive compounds, which can confer exceptional health benefits, and are consequently referred to as "superfruits" (Ciesarova et al. 2020; Lima et al. 2019; Mulati et al. 2020; Nazar et al. 2023). In recent years, the escalating pollution of cadmium (Cd), a heavy metal, poses a significantly underestimated threat to human health. Cd has extensive applications in various areas of human production and daily life, including battery manufacturing, metal smelting, the use of pesticides and fertilizers. At the same time, it can accumulate in the bodies of organisms within terrestrial and marine ecosystems, ultimately entering the human body through the food chain (Z. H. Li et al. 2023; Strungaru et al. 2018; Strungaru et al. 2017; R. Wang et al. 2023; as shown in Figure 1).

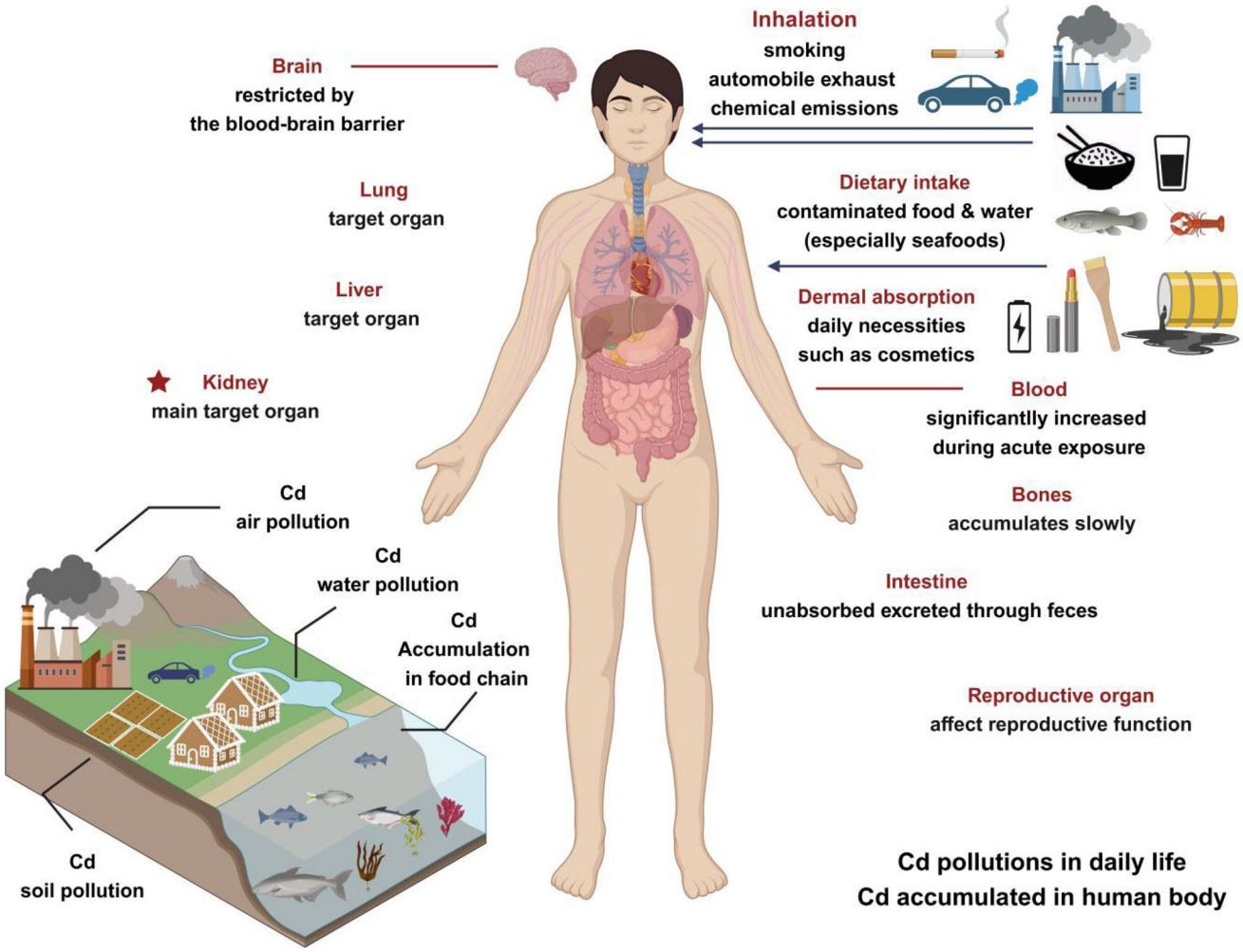

FIGURE 1 | Cadmium (Cd) pollutions in daily life and its accumulation in human body.

Cd readily interacts with proteins and enzymes within the human body, bioaccumulating in specific organs, with the kidneys and liver being particularly vulnerable target organs to its toxic effects (Kim et al. 2013; B. Wang and Du 2013; Wu et al. 2012). Studies indicate that non-occupationally exposed smokers have a daily Cd intake of approximately 2–20 μg, which significantly elevates renal Cd burden and induces marked renal impairment (Y. Liu et al. 2016). Previous studies have also demonstrated that Cd-induced renal injury is strongly associated with oxidative stress and inflammatory responses. Cd disrupts the renal antioxidant defense system by impairing total glutathione (T-GSH) levels and antioxidant enzyme activities, leading to intracellular accumulation of reactive oxygen species (ROS). This process subsequently triggers DNA strand breaks, protein denaturation, lipid peroxidation (LPO), mitochondrial membrane damage, and cellular apoptosis (Mandel et al. 2006). Furthermore, Cd stimulates excessive nitric oxide (NO) production in renal tissues. The interaction between NO and superoxide anion ($O_2^{\bullet -}$) generates potent ROS such as peroxynitrite anion ($ONOO^-$), which not only exacerbates LPO but also amplifies inflammatory cascades. These interconnected mechanisms collectively intensify oxidative stress burden and promote inflammatory damage in renal tissues, ultimately aggravating Cd-induced nephrotoxicity (R. Li et al. 2011; J. Liu et al. 2009).

In clinical practice, the primary chemical agents employed to alleviate acute Cd-induced injury include ethylenediaminetetraacetic acid (EDTA), disodium edetate, and 2,3-dimercapto-1-propanesulfonic acid (DMPS). Although these chelators demonstrate efficacy in sequestering heavy metal ions, their clinical application is limited by dose-dependent toxic side effects, particularly the induction of secondary hepatic and renal damage (Born et al. 2013; Bradberry and Vale 2009; Huang et al. 2019). Consequently, they are not suitable for routine administration as dietary supplements due to these safety concerns (Baxter and Krenzelok 2008; Lubovac-Pilav et al. 2013; Y. Wang et al. 2020). Therefore, naturally sourced and safer antioxidants have emerged as superior candidates for preventing or mitigating Cd-induced physiological damage. In recent years, numerous studies have focused on bioactive compounds of natural origin, investigating their potential efficacy in preventing or alleviating Cd toxicity at cellular and organismal levels. For instance, naringenin has been demonstrated to effectively attenuate Cd-induced KGN cell apoptosis, oxidative stress, mitochondrial dysfunction, and inflammatory responses through modulation of sirtuin-1 (SIRT1) expression (Yuan et al. 2024). Evodiamine not only activates the nuclear factor E2-related factor 2 (Nrf2)/HO-1 antioxidant pathway to mitigate Cd-induced nephrotoxicity (Song et al. 2021) but also ameliorates colonic inflammatory injury by activating

autophagy and suppressing NLRP3 inflammasome assembly (Ding et al. 2020). Epigallocatechin gallate (EGCG) in tea protects MC3T3-E1 cells against Cd-induced apoptosis and osteogenic dysfunction through modulation of the PI3K/AKT/mTOR and Nrf2/HO-1 signaling pathways. Puerarin exerts a protective mechanism in AML12 hepatocytes against Cd-induced inhibition of autophagy and activation of the NLRP3 inflammasome through the Nrf2 pathway (Wei et al. 2024). The present study investigates the potential of quercetin to protect against Cd-induced cognitive deficits in rats by modulating the downstream signaling of the PI3K/AKT-Nrf2/ARE pathways in the hippocampus (Yu et al. 2021). The extant studies demonstrate that polyphenolic compounds are naturally occurring substances, which are capable of fulfilling significant active functions.

Anthocyanins, classified as flavonoid compounds and a subclass of phenolic phytochemicals, are water-soluble pigments commonly found in fruits. These compounds exert potent antioxidant and anti-inflammatory effects primarily through the modulation of signaling pathways including NF-κB and Nrf2/Kelch-like ECH-associated protein 1 (Keap1). Current research on the alleviation of Cd-induced damage by anthocyanins primarily focuses on their role in reproductive toxicity. For instance, cyanidin-3-*O*-glucoside (C3G) has been demonstrated to ameliorate Cd-induced epithelial proliferation in murine uterine tissue (Yang et al. 2022). Anthocyanins derived from *Lycium ruthenicum* (black goji berry) alleviate Cd-induced oxidative stress and testicular toxicity through activation of the *Nrf2*/*Keap1* signaling pathway (Dong et al. 2024). Malvidin-3-*O*-glucoside ameliorates Cd-mediated cellular dysfunction in estradiol production of human granulosa cells (Liang et al. 2023).

Therefore, in the present study, we mainly focused on oxidative stress and inflammatory response pathways, collecting 11 kinds of potential "superfruits" that are likely rich in anthocyanins (including blueberry [BLUB], which is more commercially available). We compared the potential of anthocyanin extracts from different fruit sources to protect Human Kidney-2 (HK-2) cells against Cd-induced oxidative stress and inflammatory damage. The aim is to assess the exploitable value of these "superfruits" and provide evidence-based consumption guidance.

2 | Materials and Methods

2.1 | Fruit Materials

A total of 11 types of fruits were used in this study, including *Aronia melanocarpa* (Michx.) Eloit, *Padus napaulensis*, *Rhodomyrtus tomentosa* (Ait.) Hassk, *Ribes nigrum* Linn., *Schisandra chinensis* (Turcz.) Baill., *Phinia cauliflora* (Mart.) Kausel, *Solanum nigrum* Linn., *Pyracantha fortuneana* (Maxim.) Li., *Campanumoea lancifolia* (Roxb.) Merr., *Hippoohae rhamnoides* Linn. and *Vaccinium* spp. Their common names and the corresponding abbreviations used in this article are as follows: BLUB, black chokeberry (BLCB, Dalian, Liaoning Province), black currant (BLCU, Shenyang, Liaoning Province), khasi cherry (KHAC, Dehong, Yunnan Province), schisandra (SCHI, Changbai Mountain, Jilin Province), jaboticoba (JABO, Zhangzhou, Fujian Province), rose myrtle (ROSM, Qingyuan, Guangdong Province), Chinese firethorn (CHIF, Bijie, Guizhou Province), sea buckthorn (SEAB, Lvliang, Shanxi Province), spider fruit (SPIF, Chuxiong, Yunnan Province), and black nightshade (BLAN, Shaoyang, Hunan Province). Except for BLUB (OZblu), which was purchased from the local commercial market, all other fruits were collected from different regions during their maturity period and transported to the laboratory via cold chain every other day. Uniformly sized and disease-free fruits were selected for photography (as shown in Figure 2A) and stored in a refrigerator at 4°C for further experiments.

2.2 | Extraction of Fruit Anthocyanins

Accurately weighed 500 g of fresh whole fruit was added with 2 L of ethanol, which had been acidified with formic acid (0.1%, v/v). It was blended thoroughly in a homogenizer and a bag containing ice was placed in an ultrasonic cleaner to prevent temperature rise. The temperature was set to 30°C and ultrasonic extraction was performed at a frequency of 35 kHz for 0.5 h. To ensure complete extraction, it was necessary to allow the mixture to sit for a period of 12 h. Following this, the mixture was filtered through cheesecloth, and then through three layers of filter paper in order to collect the solution obtained by filtration. The filtrate was concentrated using a vacuum rotary evaporator (Heidolph, 80 rpm, at 30°C for 3–4 h). It was imperative that the entire extraction process is conducted in the dark in order to prevent the degradation of anthocyanins.

Then, the concentrated extracts were dissolved in 200–400 mL of double-distilled water, and transferred to several 50 mL centrifuge tubes. The solid-phase extraction of the anthocyanin extracts was performed using a Sep-Pak C_{18} column (12 cc, with a sample loading capacity of 2 g, Waters Corp., Milford, MA). The specific steps involved were as follows: first, the column with 1 bed volume (BV) of methanol was activated. Second, the column with 2 BV of double-distilled water was equilibrated. Next, the aqueous phase containing 0.8 BV of the sample was applied, then sugars, acids, and other impurities were removed with 20 BV of double-distilled water. Finally, the methanol eluate is subjected to concentration via vacuum centrifugation (Concentrator plus, at 30°C for 10–12 h) until it assumes a powder-like consistency. It was of paramount importance that this process is conducted in a dark environment, and the weight of the powdered extract is meticulously recorded for subsequent storage in a −20°C freezer.

2.3 | Detection and Relative Quantitative Analysis of Anthocyanin Extracts

2.3.1 | Sample Preparation

According to our previous research (J. Chen et al. 2022), we characterized the structure of fruit anthocyanins using UPLC Triple TOF/MS with slight modifications. 0.05 g of anthocyanin extracts samples was weighed and dissolved in 1 mL of chromatography grade methanol (containing 5 ‰ chromatography grade formic acid). The samples were then subjected to a process of vortexing and shaking, after which the solution was diluted 10-fold to obtain a concentration of 5 mg/mL. The solution was subjected to a centrifugal process (8000 rpm, 30 min), with the centrifuge set to a temperature of 4°C in advance to ensure that the process was

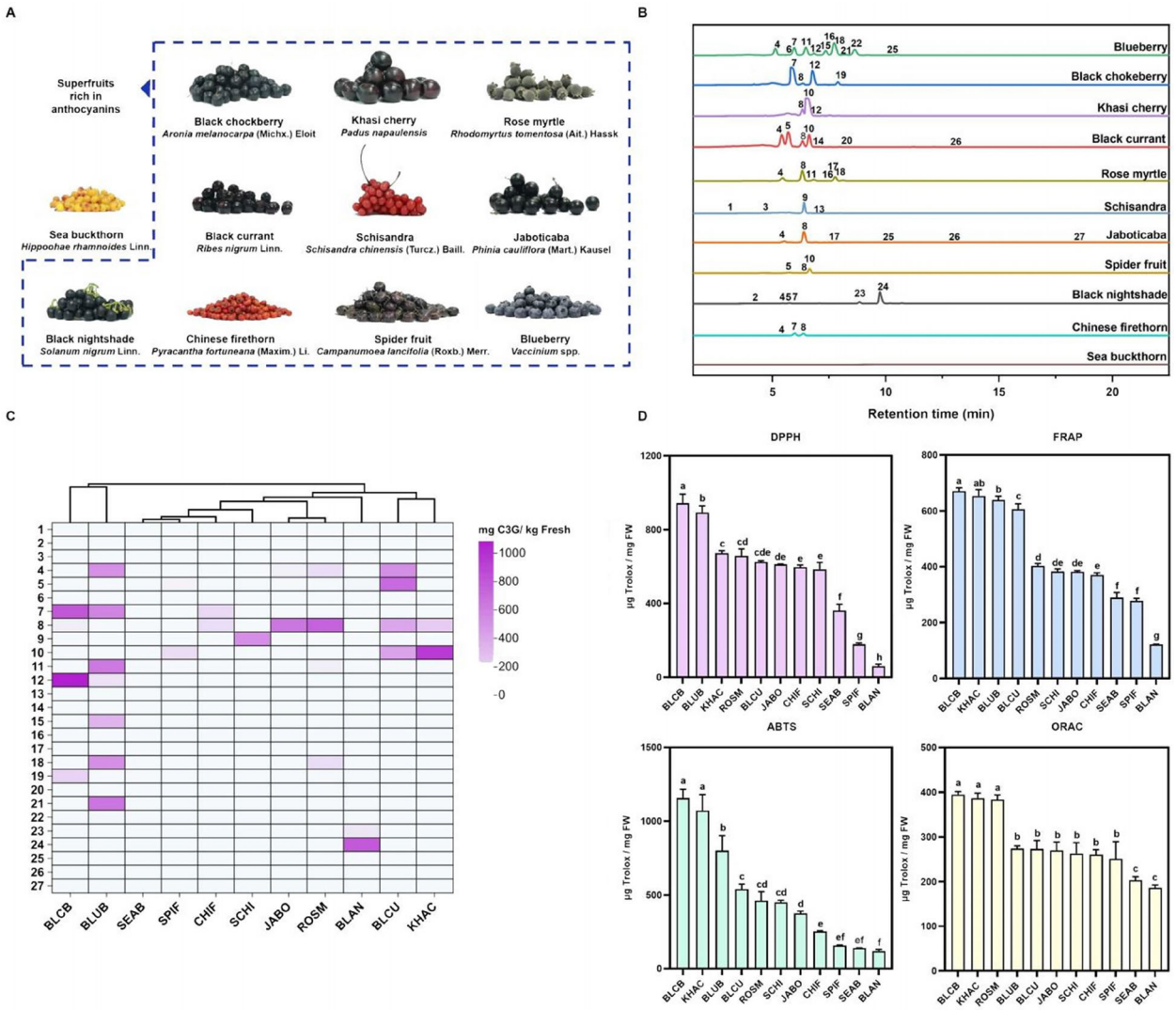

FIGURE 2 | Identification and chemical antioxidant evaluation of anthocyanin extracts from superfruits. (A) Fruit materials. (B) High-resolution mass spectrum stack of anthocyanin extracts from superfruits ($\lambda = 520$ nm). (C) Heat map of relative quantification of major anthocyanins in different super fruits. (D) Comparison of antioxidant activities of super fruits anthocyanin extracts based on DPPH, FRAP, ABTS, and ORAC in vitro. All samples are analyzed in triplicate. The error bars are expressed as mean ± SEM. Statistical significance was determined using one-way analysis of variance and multiple group comparison *t*-test. Different letters indicate statistically significant differences between groups ($p < 0.05$). The corresponding substances are as follows: 1:Cy-3-*O*-glc-rut; 2: Dp-3-*O*-sop; 3:Cy-3-*O*-sam; 4:Dp-3-*O*-gal or Dp-3-*O*-glc; 5: Dp-3-*O*-rut; 6: Dp-3-*O*-ara; 7: Cy-3-*O*-gal; 8: Cy-3-*O*-glc; 9:Cy-3-*O*-xyl-rut; 10:Cy-3-*O*-rut; 11:Pet-3-*O*-gal or Pet-3-*O*-glc; 12:Cy-3-*O*-ara; 13: Cy-3-*O*-xyl-glc; 14:Pet-3-*O*-rut; 15:Pet-3-*O*-ara; 16:Peo-3-*O*-gal or Peo-3-*O*-glc; 17:Pel-3-*O*-glc; 18: Mv-3-*O*-gal; 19:Cy-3-*O*-xyl; 20:Peo-3-*O*-rut; 21:Peo-3-*O*-ara; 22:Mv-3-*O*-ara; 23:Del-3-*O*-rut(trans-p-coumaroyl)-5-*O*-glc; 24:Pet-3-*O*-rut(cis-p-coumaroyl)-5-*O*-glc or Pet-3-*O*-rut(trans-p-coumaroyl)-5-*O*-glc; 25:Dp-3-*O*-acl; 26:Dp-3-*O*-(6-p-coumaroyl)-glc; 27: Cy-3-*O*-(6-p-coumaroyl)-glc. Abbreviations: acl, acetylglicoside; ara, arabinoside; BLCB, black chokeberry; BLCU, black currant; BLAN, black nightshade; BLUB, blueberry; CHIF, Chinese firethorn; cy, cyanidin; dp, delphinidin; gal, galactoside; glc, glucoside; JABO, jaboticaba; KHAC, khasi cherry; mv, malvidin; pel, pelargonidin; peo, peonidin; pet, petunidin; ROSM, rose myrtle; rut, rutinoside; sam, sambubioside; SCHI, schisandra; SEAB, sea buckthorn; sop, sophoroside; SPIF, spider fruit; xyl, xyloside.

carried out at a low temperature away from light. After filtering through a microporous membrane (organic system, 0.22 μm), 150 μL was taken and added to a liquid phase bottle.

2.3.2 | UPLC-MS/MS Detection

Used Waters 2695-2996 UPLC system to detect and identify anthocyanin extracts. The relevant procedures and systems were as follows: ACQUITYUPLC HSST3 (1.8 μm, 2.1 × 150 mm) liquid chromatography column was used as the stationary phase; mobile phase A and mobile phase B were 1% formic acid (v/v) water and 1% formic acid (v/v) acetonitrile, respectively. The optimized elution program was: 0/5, 15/30, 23/50, 30/95 (min/B%); sample injection volume was 3 μL; the detection wavelength was 520 nm; the column temperature was 50°C; the flow rate was 0.3 m/min. LC-MS analysis was performed on the AB Triple TOF6600 plus System (ABSCIEX, Framingham), and mass spectrometry analysis was performed in both positive and negative ion modes. The optimal parameter settings were: positive ion mode, source

voltage (+5.5 kV), source temperature (550°C), the pressure of atomizer gas 1 (air) and atomizer gas 2 (air) were set to 50 psi, the pressure of curtain gas (N2) was set to 35 psi. Moreover, the maximum allowable error was set to ± 5 ppm. De clustering potential (DP), 80 V; collision energy (CE), 10 V. For the MS/MS acquisition mode, the parameters were almost the same except for the CE set to 40 ± 20 V, ion release delay (IRD) set to 67, and ion release width (IRW) set to 25. The m/z scanning range for precursor ions and product ions was set to 100–1500 Da and 50–1500 Da, respectively. Automatically perform precise mass number calibration before each analysis using the automatic calibration conveyor system.

2.3.3 | Identification and Relative Quantitative Analysis

Chromatographic data were processed using PeakView software (version 1.2, AB SCIEX, Toronto, ON, Canada). With the help of Reaxys database (https://www.reaxys.com/), we compared the data of ion fragmentation peak with previous studies. Then utilizing C3G as the standard, the expression of other identified anthocyanins in their equivalents was conducted. Eight concentration gradients were prepared for the standard, with 10 μL being extracted for UPLC analysis. The process was the same as 2.3.2.

The construction of a standard curve was performed, with the concentration of standard samples designated as the x-axis and the cumulative peak area (geology) as the y-axis. The separation degree of C3G standard and the linear relationship were effective, with the correlation coefficient being above 0.99. Then the relative quantification of the main anthocyanin components in different fruits could be calculated based on a material-liquid ratio of 1:4. In order to more visually compare main anthocyanin substances in different superfruits, the online platform https://www.chiplot.online/ was utilized to generate a heat map, and a cluster analysis was performed (Ji et al. 2022; X. Li et al. 2023).

2.4 | In Vitro Chemical Antioxidant Capacity Evaluation

Based on the previous paper published by our research group (Y. Wang et al. 2017), four chemical antioxidant capacity evaluation experiments were utilized in this study, including 1,1-diphenyl-3-trinitrophenylhydrazine (DPPH), ferric ion reducing antioxidant power (FRAP) method, 2,2-benzyl-di-(3-ethyl-benzothiazole-6-sulfonic acid) diammonium salt (ABTS), and oxygen free radical absorption capacity (ORAC) method. Results were expressed as mg/g DW antioxidant capacity (Trolox equivalent, dry weight), with four replicates for each sample.

2.5 | HK-2 Cell Culture and Processing

2.5.1 | Cell Culture and Group Design

HK-2 cell was inoculated into DMEM-F/12 (1:1) medium (containing 10% fetal bovine serum (FBS) and 1% penicillin-streptomycin), then placed in a sterile cell culture incubator at 37°C and 5% CO_2 for monolayer culture to observe the growth status of the cells. Passage culture was performed when the cells grew to more than 80% fusion, and the cell suspension was passed into a new 10 cm dish at a 1:3 ratio.

The experimental design comprised three groups. Blank control group (CON, control): Cells were cultured in DMEM/F12 medium supplemented with 10% FBS. Cd chloride exposure group (MOD, model): $CdCl_2$ (molecular weight 183.32) was dissolved in DMEM/F12 medium, followed by adjusting the final concentrations of $CdCl_2$ to 100, 75, 60, 50, 25, and 5 μM. Anthocyanin extracts-intervened Cd exposure group: anthocyanin extracts (50 mg/mL) was fully dissolved in cell-grade dimethyl sulfoxide (DMSO) and serially diluted to prepare stock solutions at 25, 12.5, and 5 mg/mL for subsequent interventions.

2.5.2 | Handling of Cell Samples

HK-2 cells in logarithmic growth phase were digested with trypsin EDTA, collected by low-speed centrifugation (1050 rpm, 5 min), and resuspended in medium. The cells were seeded into a 96-well plate at a density of 5×10^4 cells per well and incubated overnight. The medium was discarded and incubated with different concentrations of $CdCl_2$ (final concentrations of 0, 5, 25, 50, 60, 75, 100 μM) for 18 h. At the same time, collected cells from the same period and inoculated them into 96-well plates at a density of 5×10^4 cells per well. Incubate overnight, discarded the culture medium, and added culture medium containing anthocyanin extracts of different concentrations (final concentrations of 25, 62.5, 125, 250 μg/mL) for 24 h, with three replicate wells set for each treatment. In this case, each well contains 200 μL of the solution system, that is, 1 μL of concentrated anthocyanin extract is added to 199 μL of cell medium (containing adherently grown cells). It is important to note that the concentration of the extracts after addition would be diluted 200-fold, which should be used to calculate the corresponding final concentration and the concentrated concentration of anthocyanin extracts, which would be configured.

The anthocyanin extracts, due to its minute volume addition to the co-incubation system, could rapidly and thoroughly dissolved and diffused into the cell culture medium of each well, thereby achieving complete contact with the cells and maintaining the color of the original medium. In the experiment, the wells were configured without anthocyanin extract, containing only medium and DMSO for the control test, thus effectively circumventing any experimental errors caused by the color of the anthocyanin.

2.5.3 | Cell Proliferation and Toxicity Assay

Cell viability was assessed using the cell proliferation and cytotoxicity detection kit (CCK-8, Shanghai Beyotime Biotechnology Co. Ltd., China). After the treatment period, the culture medium was removed, and the cells were washed twice with PBS. 10 μL of CCK-8 reagent was diluted in serum-free DMEM/F12 medium (1:9, v:v) and added to each well. Following a 1.5-h incubation in the dark at 37°C, the optical density values at wavelengths of 450 and 620 nm were measured using a microplate reader. DMSO was used as a blank solvent control. The data were analyzed to

calculate cell survival rates, using the following formula:

$$\text{Cell survival } (\%) = [(\text{OD}_{450} \text{ (treatment group)} - \text{OD}_{620} \text{ (treatment group)})/(\text{OD}_{450} \text{ (control group)} - \text{OD}_{620} \text{ (control group)})] \times 100\%.$$

Prior to the execution of formal experiments, an initial trial was conducted in which various gradients of anthocyanin extracts from 11 fruits were co-incubated with cells for a period of 24 h. The objective of this trial was to ascertain the appropriate safe dose, which was determined by the assessment of cell survival. The concentration that was selected was that at which cell survival reached a value greater than 80%. Simultaneously, we assessed the impact of different concentration gradients of Cd chloride on cell viability through co-incubation with the cells. The lowest induction concentration of Cd corresponding to a cell survival rate of over 60% was selected for further analysis.

2.5.4 | Establishment of Cd-induced HK-2 Cell Damage Model

According to the preliminary experimental results in 2.5.3, 60 μM was selected as the modeling concentration of $CdCl_2$, and 25 μg/mL was chosen as the final experimental concentration of anthocyanin extracts.

HK-2 cells in the logarithmic growth phase were digested with trypsin-EDTA and collected by low-speed centrifugation (1050 rpm, 5 min). After resuspending the cell pellet in the culture medium, 5×10^4 cells per well were seeded in 96-well plates and incubated overnight at 37°C in a 95% CO_2 atmosphere to allow the cells to adhere. Cells from all three experimental groups were uniformly treated and cultured for 24 h.

The control group comprised HK-2 cells maintained under standard culture conditions, with a parallel blank control group treated with DMSO to account for solvent effects. In the model group, the HK-2 cells were exposed to a medium containing 60 μM $CdCl_2$ for a duration of 24 h. For the Cd-exposed group that intervened with anthocyanin extracts, the cells were first co-incubated with a medium containing a final concentration of 25 μg/mL anthocyanin extracts for 6 h. Thereafter, the original medium was discarded and replaced with DMEM/F12 medium containing a final concentration of 60 μM $CdCl_2$. The anthocyanin extracts were added once more, made co-incubation continued for 24 h. Three replicate wells were set up for each treatment. Cell viability and other indices were determined using the method described in 2.5. The entire experiment was protected from light as much as possible.

2.5.5 | Measurement of Cytoplasmic ROS Content and NO Release

ROS levels and NO release in the cell culture solution were measured at the end of cell treatment in each group using a commercial kit (Shanghai Beyotime Biotechnology Co. Ltd., China) according to the instructions.

2.5.6 | Detection of Cellular Antioxidant Enzyme Activity and Malondialdehyde (MDA) Content

After cell treatment, both supernatant and cells were collected. The collected cell pellet was washed one to two times with PBS, then 0.3–0.5 mL PBS was added to suspend the cells. After ultrasonic fragmentation, they were assayed. Detection of antioxidant enzyme activities such as MDA and superoxide dismutase (SOD) in cells was performed using commercial reagent kits (Nanjing Jiancheng Biotechnology Co. Ltd., China) according to the instructions.

2.5.7 | Measurement of Cellular Inflammatory Factor Content

Cell treatment was as same as 2.5.6. Diluted appropriately and used enzyme-linked immunosorbent assay (ELISA) for detection. Follow the instructions of the ELISA kit (Shanghai Enzyme-linked Biotechnology Co. Ltd., China) for specific steps.

2.5.8 | Quantitative PCR Detection of Gene Expression Related to Oxidative Stress and Inflammation

In order to collect adequate cells for gene expression analysis, HK-2 cells were cultured in six-well plates. Each group of cells were treated as Section 2.5.4. After treatment, supernatants and cells were collected. Total RNA was extracted from HK-2 cells according to the instructions provided in the manual for the total RNA rapid extraction kit (Zhejiang Easy-Do biotechnology Co. Ltd., China). Following this, DNA was removed, and cDNA was synthesized by reverse transcription using a reverse transcription kit (HisScript II Q RT SuperMix for qPCR, Nanjing Vazyme Biotech Co. Ltd., China). Subsequently, dye-based fluorescence quantification premix (ChamQ Universal SYBR qPCR Master Mix, Nanjing Vazyme Biotech Co. Ltd., China) was used for qPCR detection on a CFX real-time fluorescence quantitative PCR instrument. For each experiment, six replicate wells were set up and the experiment was repeated at least three times. β-actin was used as an internal reference, and the relative gene expression was calculated using the 2-ΔΔCt method. The qRT-PCR primer sequences are shown in Tables S1 and S2.

2.5.9 | Data Processing and Analysis

Statistical analyses were performed using IBM SPSS Statistics 22 (IBM Corp., Armonk, NY). All data are presented as mean ± standard error of the mean (SEM). Alphabetical labeling (lowercase letters) was employed to concisely indicate statistically distinct subgroups ($p < 0.05$) identified through post hoc comparisons. All datasets were processed and visualized using GraphPad Prism 9.0 (GraphPad Software Inc., San Diego, CA) and OriginPro 2021b (OriginLab Corporation, Northampton, MA). Schematic diagrams were created with BioRender.com, and final figure

compositions were assembled using Microsoft PowerPoint 365 (Microsoft Corporation, Redmond, WA).

3 | Results

3.1 | Identification of the Main Components of Anthocyanin Extracts

High-resolution mass spectrometry was used to analyze the main anthocyanin components in blueberries and 10 kinds of superfruits. The UPLC spectra were stacked and merged at 520 nm into Figure 2B for presentation. Slightly adjust the retention time based on Peak 8 (C3G). The obtained mass spectrometry data were compared with published literature, and the results are shown in Table 1, including retention time, mass-to-charge ratio (m/z) data, molecular formula, and references. From these superfruits presenting different colors, a total of 27 anthocyanins were identified, covering the six most common aglycones in plant-based foods: cyanidin (m/z 287), delphinidin (m/z 303), petunidin (m/z 317), peonidin (m/z 301), pelargonidin (m/z 271), and malvidin (m/z 331).

Among the 27 anthocyanin compounds mentioned above, C3G (Peak 8) was calibrated according to its standard, while the remaining 26 anthocyanin compounds were calculated based on the equivalent of C3G. As shown in Table S3 (the vertical axis numbers of the table represent the 27 identified anthocyanins). The relative content of total anthocyanins in BLUB is the highest (3428 mg C3G/kg fresh), followed by BLCB (2145 mg C3G/kg fresh), BLCU (2104 mg C3G/kg fresh), KHAC (1198 mg C3G/kg fresh), and ROSM (1108 mg C3G/kg fresh). Meanwhile, through the simple cluster analysis of the species and content of main anthocyanins in different super fruits, we found that these groups were relatively similar: BLUB and BLCB, BLCU and KHAC, JABO and ROSM. A heat map (Figure 2C) was drawn from the data in Table S3 to provide a more visual representation of the relative quantification of the major anthocyanins in different super fruits. The darker the color, the higher the anthocyanin content in that super fruit. And the simple cluster analysis in Figure 2C showed the similarity of the anthocyanin species content of these superfruits, such as BLCU and KHAC, BLCB, and BLUB.

Considering that the types and concentrations of anthocyanins vary among different fruits, their in vitro chemical antioxidant activity provided valuable insights into the antioxidant capacity of various superfruits. The results are presented in Figure 2D. In the DPPH experiment, the antioxidant activity of superfruits anthocyanins showed significant changes between 59.88 ± 3.88 and 942.82 ± 36.73 μg Trolox/mg FW. Among them, the BLCB has the highest DPPH value, significantly different from BLUB, while BLAN has the lowest DPPH value. In the FRAP experiment, BLCB and KHAC have the highest FRAP values, and there is a significant difference between BLCB and BLUB. BLAN still has the lowest FRAP value. In the ABTS experiment, BLCB and KHAC have the highest ABTS values, both significantly higher than BLUB, while SPIF, SEAB, and BLAN have the lowest ABTS values, but the difference is not significant. In the ORAC experiment, BLCB, KHAC, and ROSM have the highest ORAC values, all significantly higher than BLUB, while SEAB and BLAN have the lowest ORAC values, with no significant difference. Overall, the antioxidant capacity of BLCB was higher than that of BLUB, and the antioxidant capacity of BLAN was the lowest.

3.2 | Effects of Anthocyanin Extracts on HK-2 Cell Survival, ROS Production, and NO Release Under $CdCl_2$ Exposure

In vitro chemical antioxidant methods often struggle to accurately replicate the complex and dynamic physiological environment, and they do not account for the ability of antioxidants to permeate cell membranes. Consequently, cell-based experiments are necessary for further exploration. Prior to establishing whether natural antioxidants can be developed into functional foods or pharmaceuticals, it is essential to conduct cytotoxicity evaluations to determine the appropriate concentration ranges.

To identify a suitable exposure concentration of $CdCl_2$, we experimentally investigated the effects of Cd exposure along with anthocyanins from superfruits across various gradient concentrations. The inhibitory activity of the extract on HK-2 cells was evaluated as shown in Figure 3A,B. As the Cd exposure concentration increased from 5 to 100 μM, the activity of HK-2 cells decreased from 96.82% ± 3.49% to 7.65% ± 0.45%. At a Cd exposure concentration of 60 μM, the survival rate of HK-2 cells was 64.91% ± 9.01%. Moreover, we observed significant differences in the effects of various anthocyanin extracts on the survival rates of HK-2 cells. High concentrations (250 μg/mL) of anthocyanin extracts from BLAN and JABO resulted in cell survival rates decreasing to approximately 20%, indicating pronounced proliferative toxicity. Conversely, at lower concentrations (25 μg/mL), the survival rates of HK-2 cells treated with all fruit anthocyanin extracts exceeded 80%. However, when co-incubated with normal HK-2 cells at a concentration of 62.5 μg/mL, the survival rates of cells treated with BLAN, JABO, and CHIF all fell below 80%, with CHIF demonstrating the most significant proliferative toxicity at this concentration. Therefore, in establishing a model of oxidative stress and inflammatory response induced by Cd on HK-2 cells, experiments were conducted using a Cd exposure concentration of 60 μM and a final concentration of anthocyanin extracts at 25 μg/mL.

The results showed (Figure 3C) that there was a significant difference in cell activity between the model group (MOD) and the control group (CON) after Cd exposure. Anthocyanin extracts from different superfruits could improve the survival rate of HK-2 cells induced by Cd to varying degrees. BLCB had a better effect on improving cell activity than BLUB, KHAC, and BLCU, but there was no significant difference. CHIF, SEAB, SPIF, and BLAN had the smallest effect on improving cell activity and no significant difference.

The increase in oxidative stress and the accumulation of ROS are key factors in Cd-induced kidney cell damage, and the level of ROS is an important indicator of cellular oxidative damage caused by normal physiological functions and environmental factors. NO is an inflammatory indicator molecule involved in various inflammatory pathological reactions. Under normal physiological conditions, ROS and NO are at relatively low levels in the body. Following exposure to Cd, as depicted in Figure 3D,E, the

TABLE 1 | Identification of fruit anthocyanins using UPLC Triple TOF/MS.

Peak no.	Retention time (min)	MS (m/z)	MS^2 ions (relative abundance) (m/z)	Molecular formula	Tentative identification	References
1	3.163	757.2182; $[M]^+$	287.0558(100) 757.2185(24.44)	$C_{33}H_{41}O_{20}$	Cyanidin-3-*O*-glucosyl-rutinoside	Liao et al. (2016), Ma et al. (2012)
2	4.11	627.1564; $[M]^+$	303.0510(100) 627.1534(10.17) 465.1029(20.34)	$C_{27}H_{31}O_{17}$	Delphinidin-3-*O*-sophoroside	Nakajima et al. (2004)
3	4.714	581.1531; $[M]^+$	287.0554(100) 581.1851(12.83) 163.0380(6.42)	$C_{26}H_{29}O_{15}$	Cyanidin-3-*O*-sambubioside	He et al. (2011)
4	5.281	465.1034; $[M]^+$	303.0513(100)	$C_{21}H_{21}O_{12}$	Delphinidin-3-*O*-galactoside or Delphinidin-3-*O*-glucoside	G. L. (Liu et al. 2012)
5	5.736	611.1626; $[M]^+$	303.0583(100) 611.1675(21.82)	$C_{27}H_{30}O_{16}$	Delphinidin-3-*O*-rutinoside	Nakajima et al. (2004), Veberic et al. (2015)
6	5.982	435.0920; $[M]^+$	303.1015(100)	$C_{20}H_{19}O_{11}$	Delphinidin-3-*O*-arabinoside	Barnes et al. (2009), J. B. Chen et al. 2022, D. Li et al. (2016)
7	6.033	449.1069; $[M]^+$	287.0552(100)	$C_{21}H_{21}O_{11}$	Cyanidin-3-*O*-galactoside	Nakajima et al. (2004)
8	6.233	449.1083; $[M]^+$	287.0566(100)	$C_{21}H_{21}O_{11}$	Cyanidin-3-*O*-glucoside	G. L. Liu et al. (2012)
9	6.436	727.2094; $[M]^+$	287.0579(100) 727.2143(34.90)	$C_{32}H_{39}O_{19}$	Cyanidin-3-*O*-xylosylrutinoside	Liao et al. (2016), Ma et al. (2012)
10	6.541	595.1664; $[M]^+$	287.0609(100) 449.1104(5.37) 595.1743(27.82)	$C_{27}H_{30}O_{15}$	Cyanidin-3-*O*-rutinoside	Nakajima et al. (2004)
11	6.669	479.1186; $[M]^+$	317.0672(100)	$C_{22}H_{23}O_{12}$	Petunidin-3-*O*-galactoside or Petunidin-3-*O*-glucoside	G. L. Liu et al. (2012)
12	6.708	419.0970; $[M]^+$	287.0554(100)	$C_{20}H_{19}O_{10}$	Cyanidin-3-*O*-arabinoside	Barnes et al. (2009), J. B. Chen et al. 2022; D. Li et al. (2016)
13	7.107	581.1725; $[M]^+$	287.0562(100) 581.1588(44.86) 301.0649(33.64)	$C_{26}H_{29}O_{15}$	Cyanidin-3-*O*-xylosyl-glucoside	Liao et al. (2016), Ma et al. (2012)
14	7.128	625.1771; $[M]^+$	317.0676(100) 625.1798(12.36)	$C_{28}H_{33}O_{16}$	Petunidin-3-*O*-rutinoside	Nakajima et al. (2004)
15	7.147	449.1072; $[M]^+$	317.0661(100)	$C_{21}H_{21}O_{11}$	Petunidin-3-*O*-arabinoside	Barnes et al. (2009), J. B. Chen et al. 2022, D. Li et al. (2016)

(Continues)

TABLE 1 | (Continued)

Peak no.	Retention time (min)	MS (m/z)	MS^2 ions (relative abundance) (m/z)	Molecular formula	Tentative identification	References
16	7.259	463.1224; [M]+	301.0712(100)	$C_{22}H_{23}O_{11}$	Peonidin-3-*O*-galactoside or Peonidin-3-*O*-glucoside	(G. L. Liu et al. (2012)
17	7.37	433.1114; $[M]^+$	271.0607(100)	$C_{21}H_{21}O_{10}$	Pelargonidin3-*O*-glucoside	Puludo et al. (2022)
18	7.725	493.1340; $[M]^+$	331.0808(100)	$C_{23}H_{25}0_{12}$	Malvidin-3-*O*-galactoside	Barnes et al. (2009), J. B. Chen et al. 2022, D. Li et al. (2016)
19	7.945	419.0977; $[M]^+$	287.0976(100)	$C_{20}H_{19}O_{10}$	Cyanidin-3-*O*-xyloside	Taheri et al. (2013), Zielinska et al. (2020)
20	8.056	609.1823; $[M]^+$	301.0723(100) 609.1848(9.85)	$C_{28}H_{33}O_{15}$	Peonidin-3-*O*-rutinoside	Nakajima et al. (2004), Veberic et al. (2015)
21	8.243	433.1225; $[M]^+$	301.0717(100)	$C_{21}H_{21}O_{10}$	Peonidin-3-*O*-arabinoside	Barnes et al. (2009), J. B. Chen et al. 2022, D. Li et al. (2016)
22	8.778	463.1226; $[M]^+$	331.0817(100) 315.0496(6.17)	$C_{22}H_{23}O_{11}$	Malvidin-3-*O*-arabinoside	Barnes et al. (2009), J. B. Chen et al. 2022, D. Li et al. (2016)
23	8.912	919.2518; $[M]^+$	303.0517(100)919.2557(60.62) 757.2017(26.11) 465.1048(15.06)	$C_{42}H_{47}O_{23}$	Delphinidin-3-O-rutinoside(trans-p-coumaroyl)-5-*O*-glucoside	Nakajima et al. (2004)
24	9.752	933.2679; $[M]^+$	317.0675 (100) 479.1203 (18.56) 711.2167 (34.45) 933.2711 (66.42)	$C_{43}H_{48}O_{23}$	Petunidin-3-*O*-rutinoside(cis-p-coumaroyl)-5-*O*-glucoside or petunidin-3-*O*-rutinoside(trans-p-coumaroyl)-5-*O*-glucoside	Nakajima et al. (2004)
25	10.261	507.0135; $[M]^+$	303.0762(100) 507.1440(25.46)	$C_{23}H_{23}O_{13}$	Delphinidin-3-*O*-acetylglicoside	Barnes et al. (2009), J. B. Chen et al. 2022, D. Li et al. (2016)
26	13.053	611.3259; $[M]^+$	303.0869(100) 611.3275(24.62) 449.1461(7.29)	$C_{30}H_{27}O_{14}$	Delphinidin-3-*O*-(6-p-coumaroyl)glucoside	Puludo et al. (2022)
27	18.626	595.2117; $[M]^+$	287.1236(100) 595.2129(54.55)	$C_{30}H_{27}O_{13}$	Cyanidin-3-*O*-(6-p-coumaroylglucoside)	Puludo et al. (2022)

Note: The corresponding substances are as follows: 1:Cy-3-*O*-glc-rut; 2: Dp-3-*O*-sop; 3:Cy-3-*O*-sam; 4:Dp-3-*O*-gal or Dp-3-*O*-glc; 5: Dp-3-*O*-rut; 6: Dp-3-*O*-ara; 7: Cy-3-*O*-gal; 8: Cy-3-*O*-glc; 9:Cy-3-*O*-xyl-rut; 10:Cy-3-*O*-rut; 11:Pet-3-*O*-gal or Pet-3-*O*-glc; 12:Cy-3-*O*-ara; 13: Cy-3-*O*-xyl-glc; 14:Pet-3-*O*-rut; 15:Pet-3-*O*-ara; 16:Peo-3-*O*-gal or Peo-3-*O*-glc; 17:Pel-3-*O*-glc; 18: Mv-3-*O*-gal; 19:Cy-3-*O*-xyl; 20:Peo-3-*O*-rut; 21:Peo-3-*O*-ara; 22:Mv-3-*O*-ara; 23:Del-3-*O*-rut(trans-p-coumaroyl)-5-*O*-glc; 24:Pet-3-*O*-rut(cis-p-coumaroyl)-5-*O*-glc or Pet-3-*O*-rut(trans-p-coumaroyl)-5-*O*-glc; 25:Dp-3-*O*-acl; 26:Dp-3-*O*-(6-p-coumaroyl)-glc; 27: Cy-3-*O*-(6-p-coumaroyl)-glc.

Abbreviations: acl: acetylglicoside; ara: arabinoside; cy: cyanidin; dp: delphinidin; gal: galactoside; glc: glucoside; mv: malvidin; pel: pelargonidin; peo: peonidin; pet: petunidin; rut: rutinoside; sam: sambubioside; sop: sophoroside; xyl: xyloside.

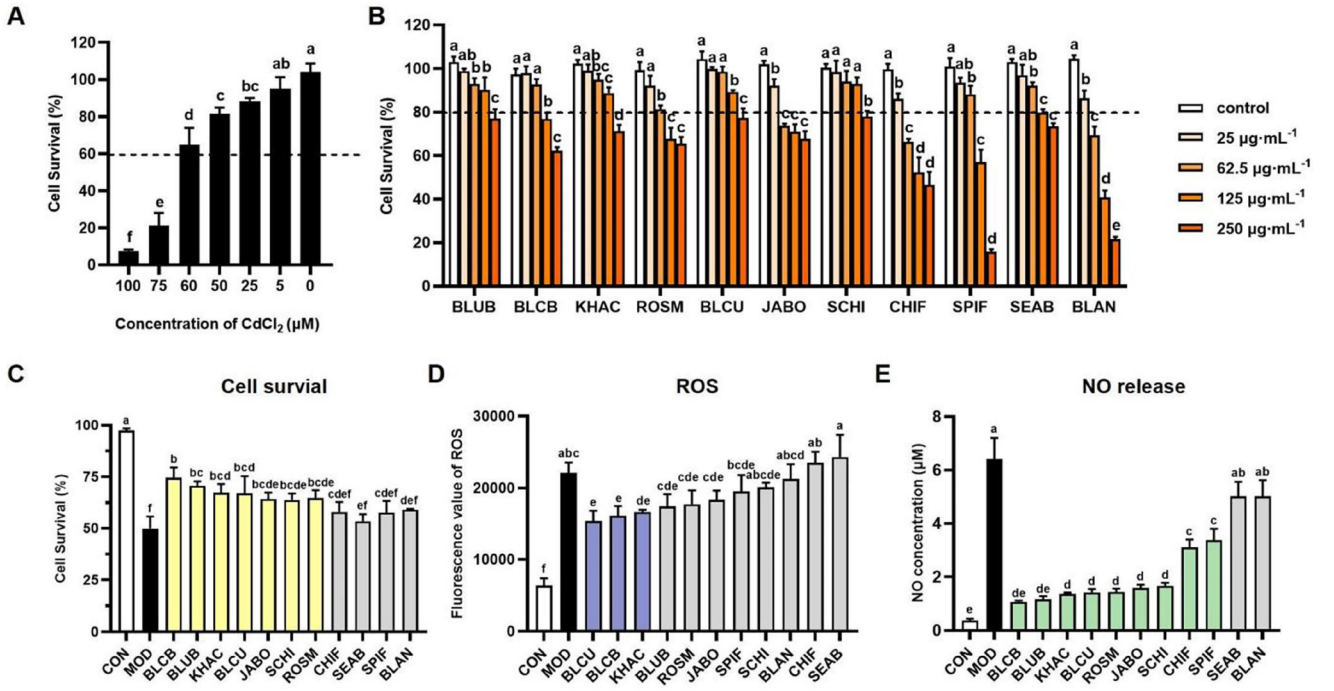

FIGURE 3 | Establishment of a HK-2 cell injury model induced by Cd exposure. (A) Evaluation of the inhibitory activity of $CdCl_2$ with different concentration gradients on HK-2 cells. The minimum Cd-induced concentration resulting in a cell viability exceeding 60% was selected as the formal experimental concentration. (B) Evaluation of the inhibitory activity of anthocyanin extracts with different concentration gradients on HK-2 cells. The minimum concentration of anthocyanin extracts resulting in a cell viability exceeding 80% was designated as the formal experimental concentration.(C-E)Compare the effects of different anthocyanin extracts on HK-2 cell activity, ROS production, and NO release under $CdCl_2$ induction. All samples are analyzed in triplicate. The error bars are expressed as mean ± SEM. Statistical significance was determined using one-way analysis of variance and multiple group comparison *t*-test. Different letters indicate statistically significant differences between groups ($p < 0.05$). Abbreviations: BLCB, black chokeberry; BLCU, black currant; BLAN, black nightshade; BLUB, blueberry; CHIF, Chinese firethorn; JABO, jaboticaba; KHAC, khasi cherry; ROSM, rose myrtle; SCHI, schisandra; SEAB, sea buckthorn; SPIF, spider fruit.

model group cells generated excessive ROS, with the differences being highly significant. Furthermore, the release of NO also increased substantially, suggesting that Cd exposure may induce considerable oxidative stress and inflammatory damage to the cells. The intervention of different anthocyanin extracts can alter the production of ROS and the release of NO in HK-2 cells under Cd exposure. Among them, BLCU, BLCB, and KHAC significantly inhibited ROS release, and all were superior to BLUB. Meanwhile, BLCB, followed by BLUB, KHAC, BLCU, ROSM, JABO, SCHI, CHIF and SPIF, all showed significant inhibitory effects on NO release, but SEAB and BLAN had no significant effects.

3.3 | Effects of Anthocyanin Extracts on Antioxidant Capacity and Oxidative Stress-related Genes of HK-2 Cells Exposed to $CdCl_2$

The effect of anthocyanin extracts on antioxidant enzyme activity and T-GSH levels in Cd-exposed cells is illustrated in Figure 4A. Compared to the control group, the activities of several antioxidant enzymes and T-GSH were significantly reduced in the model group cells, with SOD activity exhibiting the most pronounced decrease, which was statistically significant. Notably, BLCB and KHAC demonstrated significant effects in enhancing CAT enzyme activity, showing significant differences, compared to BLUB. While BLCB significantly mobilized SOD enzyme and GSH-Px enzyme activities, there were no significant differences observed when compared to BLUB. The effects of CHIF, SPIF, BLAN, and SEAB on antioxidant enzyme activity were not significant. In the assessment of T-GSH level, the effects of SPIF, SEAB, and BLAN were not significant. However, the anthocyanin extracts from other superfruits exhibited positive effects.

Results indicate that the increase in MDA level of HK-2 cells exposed to Cd was extremely significant when compared to the control group. Following intervention with anthocyanin extract, differing effects were observed in the inhibition of Cd-induced MDA production in HK-2 cells. Specifically, KHAC, BLCB, and BLCU demonstrated significant inhibitory effects, with KHAC and BLCB showing significant differences, compared to BLUB. ROSM also exhibited notable effects, while the impacts of the other superfruits were not statistically significant.

Meanwhile, as shown in Figure 4B, the effects of anthocyanin extracts on the expression of oxidative stress-related genes—including those associated with antioxidant enzymes and key factors in the classical antioxidant pathway—were investigated in HK-2 cells exposed to Cd. Compared to the control group, the model group exhibited a significant reduction in the expression of antioxidant enzyme-related genes (*Sod1, Cat, Gpx1, Gss*). The anthocyanin extracts have different effects on the expression of antioxidant enzyme-related genes. Among them, JABO can significantly increase the expression of *Cat* and *Sod1* genes, and

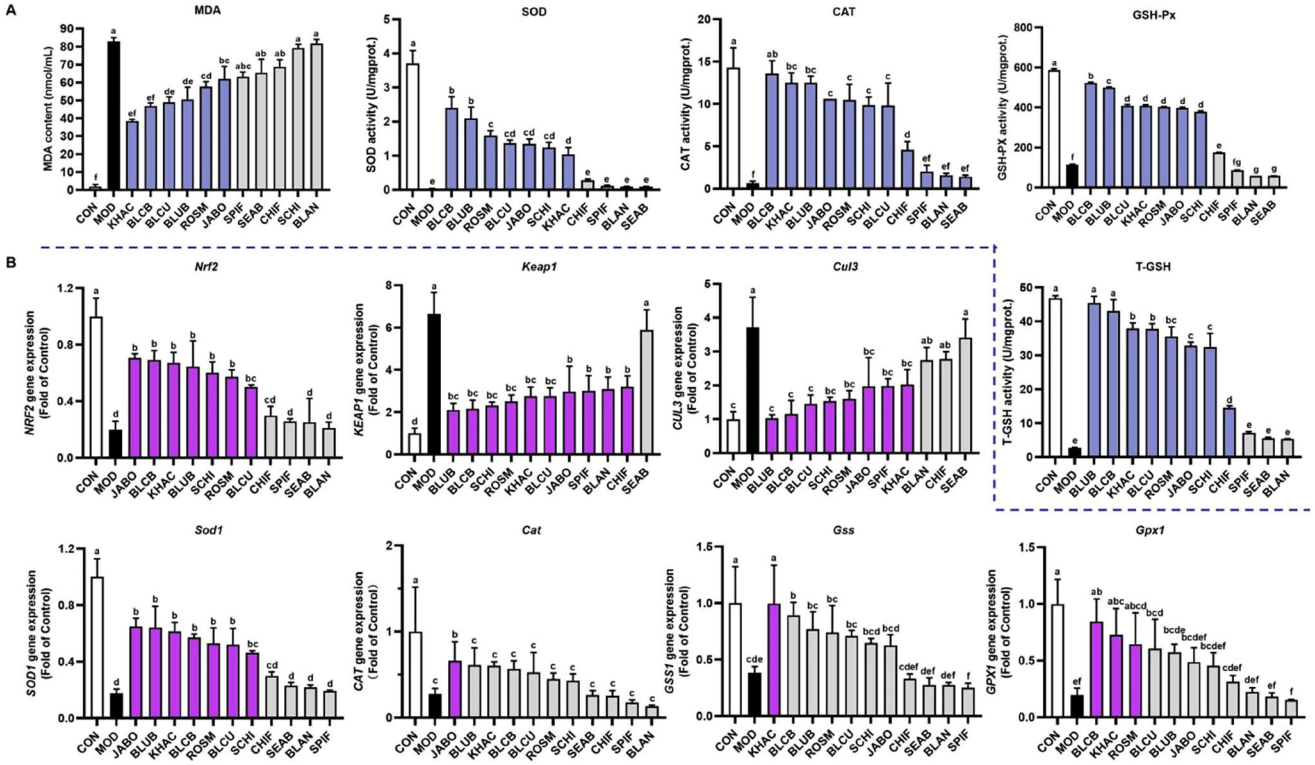

FIGURE 4 | Protective effects of anthocyanin extracts on oxidative stress damage of HK-2 cells exposed to $CdCl_2$. (A) Effects of different anthocyanin extracts on the content of peroxides MDA and antioxidant enzymes in HK-2 cells exposed to Cd. (B) The regulatory effects of different anthocyanin extracts on oxidative stress-related genes in HK-2 cells exposed to Cd. All samples are analyzed in triplicate. The error bars are expressed as mean ± SEM. Statistical significance was determined using one-way analysis of variance and multiple group comparison *t*-test. Different letters indicate statistically significant differences between groups ($p < 0.05$). Abbreviations: BLCB: black chokeberry; BLCU: black currant; BLAN: black nightshade; BLUB: blueberry; CHIF: Chinese firethorn; JABO: jaboticaba; KHAC: khasi cherry; ROSM: rose myrtle; SCHI: schisandra; SEAB: sea buckthorn; SPIF: spider fruit.

its regulatory effect on *Cat* genes is significantly different from that of BLUB. In terms of increasing *Sod1* gene expression, KHAC, BLCB, ROSM, BLCU, and CHIF also have significant effects. BLCB, KHAC, and ROSM significantly increased the expression of the *Gpx1* gene, while KHAC had a significant effect on the expression of the *Gss* gene, but BLUB had no significant regulatory effect on *Gpx1* and *Gss* genes.

The Nrf2/Keap1 signaling pathway plays a crucial role in the cellular response to oxidative stress (C. Chen et al. 2023). Compared to the control group, Cd exposure resulted in a significant decrease in *Nrf2* gene expression in HK-2 cells, accompanied by a significant increase in the expression of *Keap1* and *Cul3* genes.

In contrast, cells treated with anthocyanin extracts from superfruits exhibited an increase in *Nrf2* gene expression and a decrease in *Keap1* and *Cul3* gene expression, compared to the model group. Notably, JABO, BLCB, and KHAC significantly elevated the expression levels of the *Nrf2* gene, although there were no significant differences, compared to BLUB. Conversely, CHIF, SPIF, SEAB, and BLAN had no significant effects on *Nrf2* expression. Additionally, SEAB did not significantly impact the decrease in *Keap1* gene expression, and BLAN, CHIF, and SEAB also showed no significant effect on the decrease in *Cul3* gene expression.

Overall, BLCB and BLUB have significant regulatory effects on antioxidant enzymes and peroxides and also have significant effects on three key genes in the *Nrf2/Keap1/Cul3* antioxidant classical pathway. However, BLUB did not show significant regulatory effects on the expression of *Cat*, *Gpx1*, and *Gss* genes. On the contrary, JABO and KHAC exhibited special regulatory abilities in this regard.

3.4 | Regulatory Effects of Anthocyanin Extracts on Inflammatory Cytokines and Inflammation Related Genes in HK-2 Cells Exposed to $CdCl_2$

Constant oxidative stress can cause inflammation and damage to the body. As shown in Figure 5, we investigated the effects of anthocyanin extracts on the secretion of inflammatory factors and the expression of related genes in HK-2 cells exposed to Cd. It includes proinflammatory cytokines IL-6, IL-1β, TNF-α, *Jak2/Stat3* inflammatory stress signaling pathway associated proteins JAK2 and STAT3, and inflammasome receptor protein NLRP3.

Compared with the control group, the model group significantly increased the expression of inflammation-related factors and proteins due to the induction of Cd. After intervention with anthocyanin extracts, the expression of inflammatory factors

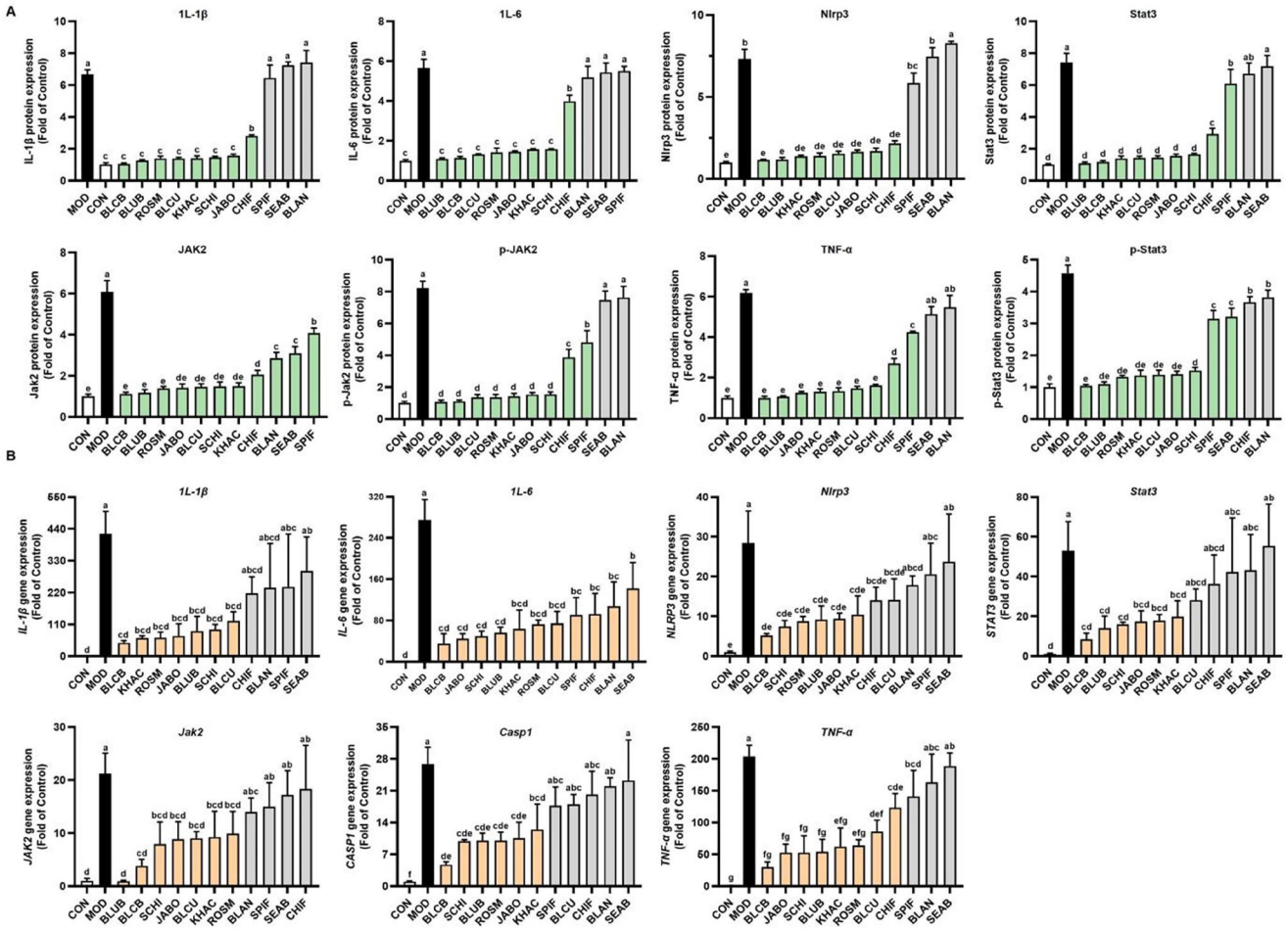

FIGURE 5 | Effects of anthocyanin extracts on inflammatory response of HK-2 cells exposed to $CdCl_2$. (A) Effects of anthocyanin extracts on the content of inflammatory factors in HK-2 cells exposed to Cd. (B) The regulatory effects of different anthocyanin extracts on inflammatory-related genes in HK-2 cells exposed to Cd. All samples are analyzed in triplicate. The error bars are expressed as mean ± SEM. Statistical significance was determined using one-way analysis of variance and multiple group comparison *t*-test. Different letters indicate statistically significant differences between groups ($p < 0.05$). Abbreviations: BLCB: black chokeberry; BLCU: black currant; BLAN: black nightshade; BLUB: blueberry; CHIF: Chinese firethorn; JABO: jaboticaba; KHAC: khasi cherry; ROSM: rose myrtle; SCHI: schisandra; SEAB: sea buckthorn; SPIF: spider fruit.

and proteins in cells was also inhibited to varying degrees. The results showed that BLCB has a significant ability to inhibit the secretion of inflammatory factors, while BLAN and SEAB have no significant effect. The results are basically consistent with the previous research. Specifically, BLCB significantly reduces the expression of *Casp1* gene, which is more effective than BLUB, ROSM, JABO, and KHAC also have significant effects. BLCB, JABO, and SCHI significantly reduced the expression of *Tnf-α* and *IL-6* genes, but the difference was not significant, compared to BLUB. SPIF, SEAB, and BLAN had no significant effect. BLCB, SCHI and ROSM significantly reduced the expression of the *Nlrp3* gene, with significant differences between BLCB and BLUB, followed by JABO and KHAC. CHIF, SPIF, SEAB, and BLAN have no significant effect on reducing *Jak2* gene expression. BLCB has a significant effect on reducing *Stat3* gene, but there is no difference, compared to BLUB. BLCB, KHAC, JABO, and ROSM have significantly better effects on reducing *IL-1β* gene expression than BLUB, followed by SCHI and BLCU.

Overall, compared with other superfruits, BLCB and BLUB have significant advantages in inhibiting the secretion of inflammatory factors and regulating the expression of genes related to inflammatory pathways. In addition, KHAC, JABO, and BLCU also have positive performance. Although SCHI is not outstanding in antioxidant and inflammatory cytokine regulation, it has shown certain potential in regulating inflammatory genes.

4 | Discussion

Cd, as an environmental toxicant, poses significant health risks to humans. The kidneys, being primary target organs for Cd accumulation, are particularly vulnerable to Cd-induced oxidative stress and inflammatory damage. In recent years, natural products have gained increasing attention as alternative therapeutic agents and nutraceutical sources for preventing and alleviating Cd-associated renal pathologies. Anthocyanins, a class of natural antioxidants with potent free radical scavenging capacity, are abundantly present in various superfruits (de Mello e Silva et al. 2022; Prakash and Baskaran 2018). Previous research has shown that the superfruit called Acai berry in the Amazon region is rich in cyanidin-3-*O*-rutinoside and C3G,

which have strong antioxidant properties and can alleviate nerve damage caused by methylmercury poisoning (Crespo-Lopez et al. 2019). However, limited research has systematically compared the protective potential of anthocyanin extracts from different superfruits against Cd-induced oxidative stress and inflammatory injury in renal cells.

In this investigation, we utilized a conventional ethanol-based extraction protocol to isolate anthocyanins from 11 superfruits. Chromatographic analysis revealed 27 distinct anthocyanin compounds across the tested specimens. Notably, SEAB exhibited no detectable anthocyanins. However, we observed that SEAB extract could also display certain performance in chemical antioxidant activity and cell viability assays. This may be attributed to the fact that anthocyanins are a subclass of flavonoids, and the extraction process may have yielded other structurally similar bioactive compounds present in SEAB. Previous studies have indicated that SEAB is rich in polyphenols, which are known to exert anti-inflammatory effects (Gore et al. 2025). Moreover, SEAB polysaccharides can play a significant role in acute intestinal inflammation in mice by modulating gut microbiota and the TRAF6/NF-κB signaling pathway (Tian et al. 2024).

By comprehensively comparing the types and contents of anthocyanins identified in other superfruits with their chemical antioxidant results and protective effects against Cd-induced damage in HK-2 cells, we found that BLCB appears to outperform BLUB (a highly commoditized fruit). This is evidenced not only by the superior antioxidant activity of BLCB but also by its significant positive effects on various metrics, including cell viability, MDA, ROS, and NO. Correlation and simple clustering analysis results (Figure 2C) further demonstrate a close relationship between the two fruits, which also bear a notable resemblance in appearance.

According to the analysis of the compounds, BLCB and BLUB were compared in terms of the types and content of anthocyanins detected. The findings indicate that BLUB has an advantage over BLCB in terms of the variety and total content of anthocyanins. However, BLCB contains a particularly prominent level of cyanidin-3-*O*-arabinoside (Peak 12), along with both them sharing the presence of cyanidin-3-*O*-galactoside (Peak 7). It is hypothesized that these two kinds of anthocyanins may possess significant potential health benefits. Notably, cyanidin-3-*O*-arabinoside has attracted attention in recent years due to studies indicating its potential anti-tumor properties from fruit sources (Zhang et al. 2022).

Furthermore, the shared compound cyanidin-3-*O*-galactoside (Peak 7) has been shown in previous studies to counteract the cytotoxic effects of tert-butyl hydroperoxide within a concentration range of 0.1 to 10 μM. It effectively reduces or completely prevents cell death, lactate dehydrogenase (LDH) release, caspase-3 activation, and DNA damage (Bellocco et al. 2016). It can also inhibit fibroblast differentiation and mitigate silica-induced pulmonary fibrosis through the Nrf2/p38/Akt/NOX4 pathway (Ma et al. 2022). Additionally, although KHAC shows less efficacy than BLUB across most indicators, a comparison reveals its antioxidant potential. The anthocyanin profile indicates that cyanidin-3-*O*-rutinoside is the most abundant in KHAC (Peak 10). Similar studies have shown that 250 μg/mL cyanidin-3-*O*-rutinoside exhibits inhibitory effects on LPO (Mulabagal et al. 2009).

Moreover, the potential of BLAN to exert effects is not particularly pronounced, which may be attributed to its unique anthocyanin composition, distinct from that of other superfruits. We detected a relatively high content of petunidin-3-*O*-rut(*cis-p-coumaroyl*)-5-*O*-glc (Peak 24) in BLAN. Due to its specific structure and the high cost of its monomer, research on its bioactivity may be limited. Furthermore, cell experiment results indicate that high doses of BLAN exhibit significant proliferative toxicity in HK-2 cells, suggesting that dosage control is necessary during application. However, there is growing interest among researchers in the pharmacological effects of BLAN and its potential health benefits. Studies indicate that BLAN contains a considerable amount of alkaloids and possesses activities such as antimalarial and hepatoprotective effects (Okokon et al. 2022). Thus, although the anthocyanin extracts from some superfruits do not demonstrate particularly remarkable effects in this study, the potential presence of other bioactive compounds and health benefits merits further exploration.

Antioxidant and anti-inflammatory activities are fundamental pathways for enhancing overall health. In addition to the classic antioxidant pathway Nrf2/Keap1 mentioned earlier, research indicates that *Nrf2* deficiency exacerbates renal injury induced by subacute Cd exposure in mice (C. Chen et al. 2021), it also protects mice from renal fibrosis induced by $CdCl_2$ exposure (C. Chen et al. 2023). These studies indicate that *Nrf2* may be a key target in addressing Cd-induced tissue damage. The activation of *Nrf2*-mediated antioxidant pathways by natural antioxidants primarily occurs through the disruption of the interaction between *Keap1* and *Nrf2*, which promotes *Nrf2* phosphorylation and prevents its ubiquitination (Fernando et al. 2019). This is similar to the effects exhibited by anthocyanin extracts in this study (Figure 6). Simultaneously, correlation heat map analysis was performed on the study indicators (Figure S1). The analysis revealed a significant positive correlation between superfruit anthocyanin extract and SOD enzyme activity ($p < 0.01$) and a significant negative correlation with IL-6 protein expression ($p < 0.01$). The relative total content of anthocyanin extracts from various superfruits showed a significant positive correlation with chemical antioxidant levels and was significantly associated with oxidative stress and inflammation-related factors, including ROS and NO. The correlation heat map demonstrates a strong association between oxidative stress and inflammation-related factors with key target proteins, providing certain references for the potential mechanisms by which superfruit anthocyanin extracts may alleviate oxidative stress and inflammatory damage.

In addition to the classic antioxidant pathway Nrf2/Keap1 mentioned earlier (Lucky et al. 2024), the *Jak/Stat* signaling pathway has been discovered in recent years as a signal transduction pathway that can regulate immunity and inflammation through cytokines (Paithankar et al. 2021). During oxidative stress, the production of NO usually increases, and in some cases, the production of NO can lead to an increase in ROS production, stimulating the activation of inflammasomes. NLRP3 is a core inflammasome mediated by *Caspase1*, which can promote the release of factors such as 1L-1β after activation (Simsek et al. 2023). JAK2, STAT3, and NLRP3 inflammasomes are significant

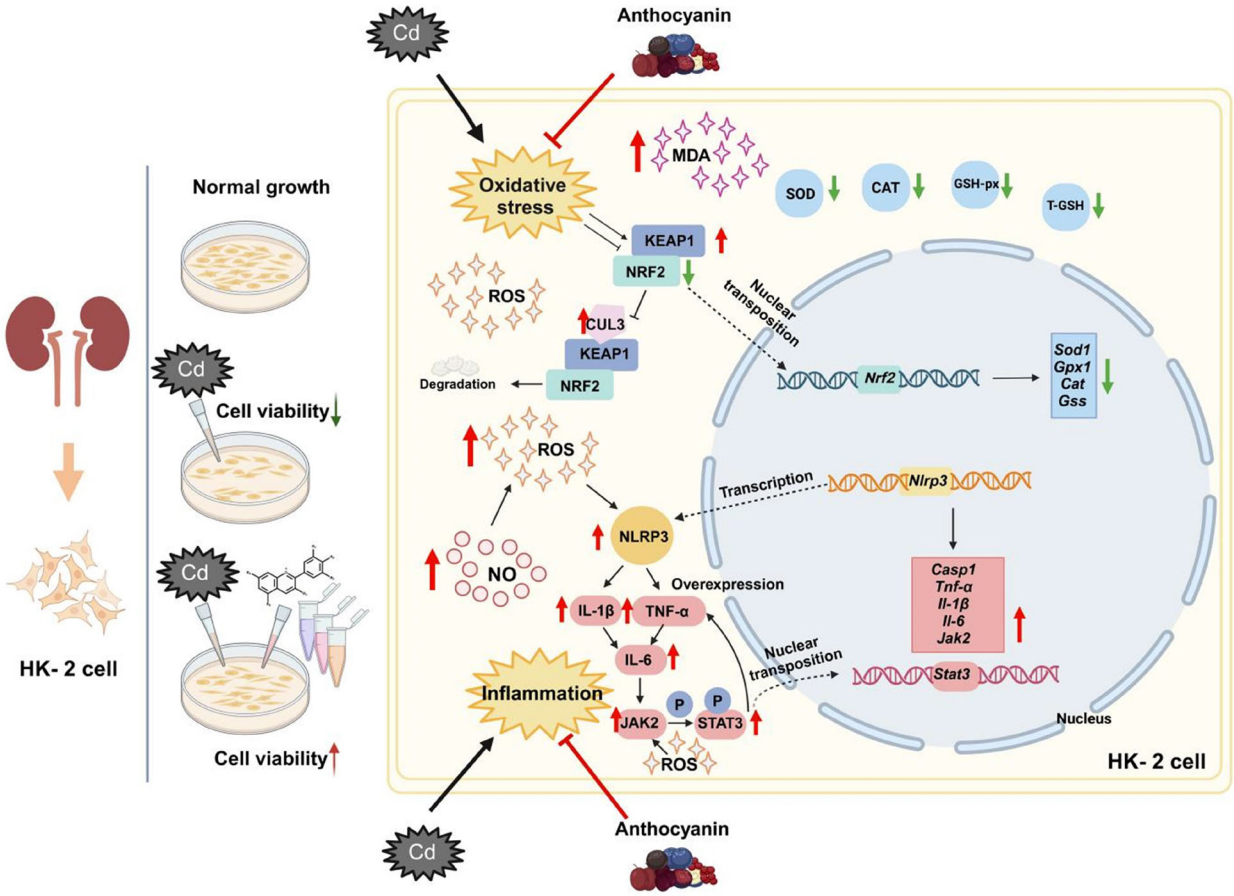

FIGURE 6 | Analysis of the possible mechanisms of anthocyanin extracts in alleviating Cd-mediated oxidative stress and inflammatory pathways in HK-2 cells.

factors and proteins related to inflammation evaluated herein. Previous studies have indicated that the JAK2/STAT3 signaling pathway and the *Klotho* gene play roles in Cd-induced neurotoxicity both in vitro and in vivo (S. Liu et al. 2023). Moreover, Cd-induced pyroptosis in SH-SY5Y cells is mediated by the PERK/TXNIP/NLRP3 signaling pathway. These studies also indicate that the oxidative stress and inflammation-related factors we examined are closely associated with Cd-induced damage and are relatively representative.

However, multiple studies have shown that Cd-induced injury is also linked to more novel pathways, such as apoptosis, autophagy, and ferroptosis. Research has demonstrated that didymin can mitigate Cd-induced renal damage by regulating the *Nrf2/Keap1* pathway, as well as influencing apoptosis, inflammation, and oxidative stress (Hamza et al. 2025). Ellagic acid alleviates Cd exposure-induced apoptosis in HT22 cells by activating the *Nrf2*/HO-1 pathway through the inhibition of oxidative stress and mitochondrial dysfunction (Y. Liu et al. 2024). Endoplasmic reticulum stress-mediated autophagy activation is implicated in Cd-induced ferroptosis in renal tubular epithelial cells (Zhao et al. 2021).

In addition, our study only evaluated the potential effects of different anthocyanin extracts in vitro. Given the more complex in vivo environment, further research is needed to explore their effects and mechanisms of action against Cd-induced tissue damage through in vivo experiments and various pathways, thereby broadening the scope of the investigation.

The fruit materials used in the investigation, with the exception of BLUB, which is highly commercialized, are largely unfamiliar to the general public. For example, KHAC, now mostly wild, is a stone fruit mainly distributed in Yunnan Province, Guizhou Province, Shaanxi Province in China and other countries, especially India (Rymbai et al. 2016). KHAC in the Chinese folk is called "rouge fruit" because its mature fruit is deep purple or purple black. BLCB, native to North America, is a cherry-shaped dark colored berry. In recent years, its enormous potential for health promotion has received more attention. It has been processed into dietary supplements such as soy sauce and fruit tea in the food industry (Sidor et al. 2019). We found that BLCB, KHAC, and BLCU may have better potential to alleviate oxidative stress and inflammatory damage induced by Cd in HK-2 cells. Therefore, there is potential for developing dietary supplements or functional foods based on these superfruits in future.

5 | Conclusion

In this study, we collected 11 kinds of superfruits and characterized their major anthocyanin profiles using UPLC-Triple-TOF/MS, with quantification of relative anthocyanin contents. The chemical antioxidant capacities of these extracts were evalu-

ated through four standardized in vitro assays. Cd-induced injury cell model was established in human renal tubular epithelial cells (HK-2) to investigate the protective effects of anthocyanin extracts, focusing on the Nrf2/Keap1 oxidative stress pathway and inflammatory mediators. Multi-dimensional analyses were performed to assess chemical antioxidant capacities, cellular viability, gene expression and protein regulation.

Results demonstrated that anthocyanin extracts from superfruit significantly enhanced cell survival rates, reduced oxidative stress markers (ROS and MDA), suppressed NO release, activated antioxidant enzymes (e.g., SOD), elevated T-GSH levels, and modulated the Nrf2/Keap1/Cul3 pathway by downregulating *Keap1* (KEAP1) and *Cul3* (CUL3) expression while upregulating *Nrf2* (NRF2) expression. Concurrently, these extracts attenuated inflammatory responses by downregulating key mediators, including IL-6, IL-1β, TNF-α, STAT3, JAK2, CASP1 and NLRP3, thereby inhibiting inflammasome activation. Among the tested superfruits, commercialized BLUB, BLCB, and KHAC exhibited the most pronounced protective effects, followed by BLCU and ROSM.

This study may provide a systematic evaluation of natural anthocyanins in mitigating Cd-induced nephrotoxicity and offer valuable insights for developing superfruit-derived interventions against environmental heavy metal Cd toxicity.

Acknowledgments

This article was supported by the National Natural Science Foundation of China (32101932) and Zhejiang Province Natural Science Foundation Joint Fund Project (LHZSD24C150001).

Conflicts of Interest

The authors declare no conflicts of interest.

Data Availability Statement

The data that supports the findings of this study are available in the supplementary material of this article.

References

Barnes, J. S., H. P. Nguyen, S. Shen, and K. A. Schug. 2009. "General Method for Extraction of Blueberry Anthocyanins and Identification Using High Performance Liquid Chromatography-Electrospray Ionization-Ion Trap-Time of Flight-Mass Spectrometry." *Journal of Chromatography A* 1216, no. 23: 4728–4735. https://doi.org/10.1016/j.chroma.2009.04.032.

Baxter, A. J., and E. P. Krenzelok. 2008. "Pediatric Fatality Secondary to EDTA Chelation." *Clinical Toxicology* 46, no. 10: 1083–1084. https://doi.org/10.1080/15563650701261488.

Bellocco, E., D. Barreca, G. Lagana, et al. 2016. "Cyanidin-3-*O*-Galactoside in Ripe *Pistachio* (L. Variety Bronte) Hulls: Identification and Evaluation of Its Antioxidant and Cytoprotective Activities." *Journal of Functional Foods* 27: 376–385. https://doi.org/10.1016/j.jff.2016.09.016.

Born, T., C. N. Kontoghiorghe, A. Spyrou, A. Kolnagou, and G. J. Kontoghiorghes. 2013. "EDTA Chelation Reappraisal Following New Clinical Trials and Regular Use in Millions of Patients: Review of Preliminary Findings and Risk/Benefit Assessment." *Toxicology Mechanisms and Methods* 23, no. 1: 11–17. https://doi.org/10.3109/15376516.2012.730562.

Bradberry, S., and A. Vale. 2009. "A Comparison of Sodium Calcium Edetate (Edetate Calcium Disodium) and Succimer (DMSA) in the Treatment of Inorganic Lead Poisoning." *Clinical Toxicology* 47, no. 9: 841–858. https://doi.org/10.3109/15563650903321064.

Chen, C., X. Han, G. Wang, et al. 2021. "*Nrf2* deficiency Aggravates the Kidney Injury Induced by Subacute Cadmium Exposure in Mice." *Archives of Toxicology* 95, no. 3: 883–893. https://doi.org/10.1007/s00204-020-02964-3.

Chen, C., Z. Zhou, S. Yu, et al. 2023. "Nrf2 protects Against Renal Fibrosis Induced by Chronic Cadmium Exposure in Mice." *Food and Chemical Toxicology* 178: 113875. https://doi.org/10.1016/j.fct.2023.113875.

Chen, J., Y. Shu, Y. Chen, et al. 2022. "Evaluation of Antioxidant Capacity and Gut Microbiota Modulatory Effects of Different Kinds of Berries." *Antioxidants* 11, no. 5: 1020. https://doi.org/10.3390/antiox11051020.

Ciesarova, Z., M. Murkovic, K. Cejpek, et al. 2020. "Why Is Sea Buckthorn (*Hippophae rhamnoides* L.) so Exceptional? A Review." *Food Research International* 133: 109170. https://doi.org/10.1016/j.foodres.2020.109170.

Crespo-Lopez, M. E., E. S. Soares, B. d. M. Macchi, et al. 2019. "Towards Therapeutic Alternatives for Mercury Neurotoxicity in the Amazon: Unraveling the Pre-Clinical Effects of the Superfruit Acai (*Euterpe oleracea*, Mart.) as Juice for Human Consumption." *Nutrients* 11, no. 11: 2585. https://doi.org/10.3390/nu11112585.

de Mello e Silva, G. N., E. S. B. Rodrigues, I. Y. L. de Macedo, et al. 2022. "Blackberry Jam Fruit (*Randia formosa* (Jacq.) K. Schum): An Amazon Superfruit With *In Vitro* Neuroprotective Properties." *Food Bioscience* 50: 102084. https://doi.org/10.1016/j.fbio.2022.102084.

Ding, W., Z. Ding, Y. Wang, et al. 2020. "Evodiamine Attenuates Experimental Colitis Injury via Activating Autophagy and Inhibiting NLRP3 Inflammasome Assembly." *Frontiers in Pharmacology* 11: 573870. https://doi.org/10.3389/fphar.2020.573870.

Dong, M., J. Lu, H. Xue, et al. 2024. "Anthocyanins From *Lycium ruthenicum* Murray Mitigate Cadmium-Induced Oxidative Stress and Testicular Toxicity by Activating the Keap1/Nrf2 Signaling Pathway." *Pharmaceuticals* 17, no. 3: 322. https://doi.org/10.3390/ph17030322.

Fernando, W., H. P. V. Rupasinghe, and D. W. Hoskin. 2019. "Dietary Phytochemicals With Anti-Oxidant and Pro-Oxidant Activities: A Double-Edged Sword in Relation to Adjuvant Chemotherapy and Radiotherapy?" *Cancer Letters* 452: 168–177. https://doi.org/10.1016/j.canlet.2019.03.022.

Gore, D. D., N. Mishra, D. Kumar, et al. 2025. "Anti-Inflammatory Activity, Stability, Bioavailability and Toxicity Studies on Seabuckthorn Polyphenol Enriched Fraction and Its Phospholipid Complex (Phytosomes) Preparation." *International Journal of Biological Macromolecules* 297: 139919. https://doi.org/10.1016/j.ijbiomac.2025.139919.

Hamza, A., S. S. F. Zadi, M. Z. Salar, M. U. Ijaz, K. A. Al-Ghanim, and A. Ishtiaq. 2025. "Mitigative Effects of Didymin Against Cadmium-Induced Renal Injury via Regulating Nrf-2/Keap-1, Apoptosis, Inflammation and Oxidative Stress." *Journal of Trace Elements in Medicine and Biology* 88: 127597. https://doi.org/10.1016/j.jtemb.2025.127597.

He, Q., Y. Shen, M. Wang, et al. 2011. "Natural Variation in Petal Color in *Lycoris longituba* Revealed by Anthocyanin Components." *PLoS ONE* 6, no. 8: e22098. https://doi.org/10.1371/journal.pone.0022098.

Huang, Y. N., F. M. Mo, J. P. Zou, et al. 2019. "A Comparative Study of the Calcium Carbonate Nanoparticles and the Chelators on Blood Lead Level Reduction and the Side Effects." *Nanoscience and Nanotechnology Letters* 11, no. 8: 1145–1152. https://doi.org/10.1166/nnl.2019.2988.

Ji, X., J. Tang, and J. Zhang. 2022. "Effects of Salt Stress on the Morphology, Growth and Physiological Parameters of *Juglans microcarpa* L. Seedlings." *Plants* 11, no. 18: 2381. https://doi.org/10.3390/plants11182381.

Kim, B. M., S. Y. Lee, and I. H. Jeong. 2013. "Influence of Squid Liver Powder on Accumulation of Cadmium in Serum, Kidney and Liver of Mice." *Preventive Nutrition and Food Science* 18, no. 1: 1–10. https://doi.org/10.3746/pnf.2013.18.1.001.

Li, D., X. Meng, and B. Li. 2016. "Profiling of Anthocyanins From Blueberries Produced in China Using HPLC-DAD-MS and Exploratory Analysis by Principal Component Analysis." *Journal of Food Composition and Analysis* 47: 1–7. https://doi.org/10.1016/j.jfca.2015.09.005.

Li, R., C. Yuan, C. Dong, S. Shuang, and M. M. Choi. 2011. "*In Vivo* Antioxidative Effect of Isoquercitrin on Cadmium-Induced Oxidative Damage to Mouse Liver and Kidney." *Naunyn-Schmiedebergs Archives of Pharmacology* 383, no. 5: 437–445. https://doi.org/10.1007/s00210-011-0613-2.

Li, X., J. Li, Q. Zhao, L. Qiao, L. Wang, and C. Yu. 2023. "Physiological, Biochemical, and Genomic Elucidation of the *Ensifer adhaerens* M8 Strain With Simultaneous Arsenic Oxidation and Chromium Reduction." *Journal of Hazardous Materials* 441: 129862. https://doi.org/10.1016/j.jhazmat.2022.129862.

Li, Z. H., Y. Shi, Y. G. Wang, et al. 2023. "Cadmium-Induced Pyroptosis Is Mediated by PERK/TXNIP/NLRP3 Signaling in SH-SY5Y Cells." *Environmental Toxicology* 38, no. 9: 2219–2227. https://doi.org/10.1002/tox.23861.

Liang, S. R., X. S. Li, R. J. Liu, et al. 2023. "Malvidin-3-*O*-Glucoside Ameliorates Cadmium-Mediated Cell Dysfunction in the Estradiol Generation of Human Granulosa Cells." *Nutrients* 15, no. 3: 753. https://doi.org/10.3390/nu15030753.

Liao, J., J. Zang, F. Yuan, et al. 2016. "Identification and Analysis of Anthocyanin Components in Fruit Color Variation in Schisandra chinensis." *Journal of the Science of Food and Agriculture* 96, no. 9: 3213–3219. https://doi.org/10.1002/jsfa.7503.

Lima, R. D. S., S. R. S. Ferreira, L. Vitali, and J. M. Block. 2019. "May the Superfruit Red Guava and Its Processing Waste be a Potential Ingredient in Functional Foods?" *Food Research International* 115: 451–459. https://doi.org/10.1016/j.foodres.2018.10.053.

Liu, G. L., H. H. Guo, and Y. M. Sun. 2012. "Optimization of the Extraction of Anthocyanins From the Fruit Skin of *Rhodomyrtus tomentosa* (Ait.) Hassk and Identification of Anthocyanins in the Extract Using High-Performance Liquid Chromatography-Electrospray Ionization-Mass Spectrometry (HPLC-ESI-MS)." *International Journal of Molecular Sciences* 13, no. 5: 6292–6302. https://doi.org/10.3390/ijms13056292.

Liu, J., W. Qu, and M. B. Kadiiska. 2009. "Role of Oxidative Stress in Cadmium Toxicity and Carcinogenesis." *Toxicology and Applied Pharmacology* 238, no. 3: 209–214. https://doi.org/10.1016/j.taap.2009.01.029.

Liu, S., D. Yu, P. Wei, et al. 2023. "JAK2/STAT3 Signaling Pathway and *Klotho* Gene in Cadmium-Induced Neurotoxicity *in Vitro* and *in Vivo*." *Biological Trace Element Research* 201, no. 6: 2854–2863. https://doi.org/10.1007/s12011-022-03370-9.

Liu, Y., C. H. Chen, Z. H. Hao, J. Z. Shen, S. S. Tang, and C. S. Dai. 2024. "Ellagic Acid Reduces Cadmium Exposure-Induced Apoptosis in HT22 Cells via Inhibiting Oxidative Stress and Mitochondrial Dysfunction and Activating Nrf2/HO-1 Pathway." *Antioxidants* 13, no. 11: 1296. https://doi.org/10.3390/antiox13111296.

Liu, Y., K. Liu, Y. Li, et al. 2016. "Cadmium Contamination of Soil and Crops Is Affected by Intercropping and Rotation Systems in the Lower Reaches of the Minjiang River in South-Western China." *Environmental Geochemistry and Health* 38, no. 3: 811–820. https://doi.org/10.1007/s10653-015-9762-4.

Lubovac-Pilav, Z., D. M. Borràs, E. Ponce, and M. C. Louie. 2013. "Using Expression Profiling to Understand the Effects of Chronic Cadmium Exposure on MCF-7 Breast Cancer Cells." *PLoS ONE* 8, no. 12: e84646. https://doi.org/10.1371/journal.pone.0084646.

Lucky, I. O., I. I. Aisuhuehien, and M. E. Adejoke. 2024. "Renoprotective Effect of Hyperin Against $CdCl_2$ Prompted Renal Damage by Activation of Nrf-2/Keap-1 ARE Pathway in Male Mice." *Toxicology Mechanisms and Methods* 34, no. 6: 717–726. https://doi.org/10.1080/15376516.2024.2329655.

Ma, C., M. Y. Lyu, C. L. Deng, et al. 2022. "Cyanidin-3-Galactoside Ameliorates Silica-Induced Pulmonary Fibrosis by Inhibiting Fibroblast Differentiation via Nrf2/p38/Akt/NOX4." *Journal of Functional Foods* 92: 105034. https://doi.org/10.1016/j.jff.2022.105034.

Ma, C., L. Yang, F. Yang, W. Wang, C. Zhao, and Y. Zu. 2012. "Content and Color Stability of Anthocyanins Isolated From *Schisandra chinensis* Fruit." *International Journal of Molecular Sciences* 13, no. 11: 14294–14310. https://doi.org/10.3390/ijms131114294.

Mandel, S., T. Amit, L. Reznichenko, O. Weinreb, and M. B. Youdim. 2006. "Green Tea Catechins as Brain-Permeable, Natural Iron Chelators-Antioxidants for the Treatment of Neurodegenerative Disorders." *Molecular Nutrition & Food Research* 50, no. 2: 229–234. https://doi.org/10.1002/mnfr.200500156.

Mulabagal, V., G. A. Lang, D. L. DeWitt, S. S. Dalavoy, and M. G. Nair. 2009. "Anthocyanin Content, Lipid Peroxidation and Cyclooxygenase Enzyme Inhibitory Activities of Sweet and Sour Cherries." *Journal of Agricultural and Food Chemistry* 57, no. 4: 1239–1246. https://doi.org/10.1021/jf8032039.

Mulati, A., S. Ma, H. Zhang, et al. 2020. "Sea-Buckthorn Flavonoids Alleviate High-Fat and High-Fructose Diet-Induced Cognitive Impairment by Inhibiting Insulin Resistance and Neuroinflammation." *Journal of Agricultural and Food Chemistry* 68, no. 21: 5835–5846. https://doi.org/10.1021/acs.jafc.0c00876.

Nakajima, J. I., I. Tanaka, S. Seo, M. Yamazaki, and K. Saito. 2004. "LC/PDA/ESI-MS Profiling and Radical Scavenging Activity of Anthocyanins in Various Berries." *Journal of Biomedicine and Biotechnology* 2004, no. 5: 241–247. https://doi.org/10.1155/S1110724304404045.

Nazar, M. S., M. B. Malgorzata, R. Joanna, and H. Tomasz. 2023. "The Protective Potential of *Aronia melanocarpa* L. Berry Extract Against Cadmium-Induced Kidney Damage: A Study in an Animal Model of Human Environmental Exposure to this Toxic Element." *International Journal of Molecular Sciences* 24, no. 14: 11647. https://doi.org/10.3390/ijms241411647.

Okokon, J. E., I. C. Etuk, P. S. Thomas, F. P. Drijfhout, T. D. W. Claridge, and W. W. Li. 2022. "*In Vivo* Antihyperglycaemic and Antihyperlipidemic Activities and Chemical Constituents of *Solanum anomalum*." *Biomedicine & Pharmacotherapy* 151: 113153. https://doi.org/10.1016/j.biopha.2022.113153.

Paithankar, J. G., S. Saini, S. Dwivedi, A. Sharma, and D. K. Chowdhuri. 2021. "Heavy Metal Associated Health Hazards: An Interplay of Oxidative Stress and Signal Transduction." *Chemosphere* 262: 128350. https://doi.org/10.1016/j.chemosphere.2020.128350.

Prakash, A., and R. Baskaran. 2018. "Acerola, an Untapped Functional Superfruit: A Review on Latest Frontiers." *Journal of Food Science and Technology* 55, no. 9: 3373–3384. https://doi.org/10.1007/s13197-018-3309-5.

Puludo, M. C., S. B. Piamental de Olivira, L. F. de Oliveira, et al. 2022. "Phenolic Composition of Peels From Different Jaboticaba Species Determined by HPLC-DAD-ESI/MS^n and Antiproliferative Activity in Tumor Cell Lines." *Current Plant Biology* 29: 100233. https://doi.org/10.1016/j.cpb.2021.100233.

Rymbai, H., A. R. Roy, N. A. Deshmukh, et al. 2016. "Analysis Study on Potential Underutilized Edible Fruit Genetic Resources of the Foothills Track of Eastern Himalayas." *India. Genetic Resources and Crop Evolution* 63, no. 1: 125–139. https://doi.org/10.1007/s10722-015-0342-3.

Sidor, A., A. Drozdzynska, and A. Gramza-Michalowska. 2019. "Black Chokeberry (*Aronia melanocarpa*) and Its Products as Potential Health-Promoting Factors—An Overview." *Trends in Food Science & Technology* 89: 45–60. https://doi.org/10.1016/j.tifs.2019.05.006.

Simsek, H., N. Akaras, C. Gur, S. Kucukler, and F. M. Kandemir. 2023. "Beneficial Effects of Chrysin on Cadmium-Induced Nephrotoxicity in Rats: Modulating the Levels of Nrf2/HO-1, RAGE/NLRP3, and Caspase-3/Bax/Bcl-2 Signaling Pathways." *Gene* 875: 147502. https://doi.org/10.1016/j.gene.2023.147502.

Song, Z. C., W. Wang, X. R. Zhang, et al. 2021. "Evodiamine Attenuates Cadmium-Induced Nephrotoxicity Through Activation of Nrf2/HO-1 Pathway." *Tropical Journal of Pharmaceutical Research* 20, no. 8: 1579–1584. https://doi.org/10.4314/tjpr.v20i8.5.

Strungaru, S. A., M. Nicoara, C. Teodosiu, E. Baltag, C. Ciobanu, and G. Plavan. 2018. "Patterns of Toxic Metals Bioaccumulation in a Cross-Border Freshwater Reservoir." *Chemosphere* 207: 192–202. https://doi.org/10.1016/j.chemosphere.2018.05.079.

Strungaru, S. A., M. Nicoara, C. Teodosiu, D. Micu, and G. Plavan. 2017. "Toxic Metals Biomonitoring Based on Prey-Predator Interactions and Environmental Forensics Techniques: A Study at the Romanian-Ukraine Cross Border of the Black Sea." *Marine Pollution Bulletin* 124, no. 1: 321–330. https://doi.org/10.1016/j.marpolbul.2017.07.052.

Taheri, R., B. A. Connolly, M. H. Brand, and B. W. Bolling. 2013. "Underutilized Chokeberry (*Aronia melanocarpa, Aronia arbutifolia, Aronia prunifolia*) Accessions Are Rich Sources of Anthocyanins, Flavonoids, Hydroxycinnamic Acids, and Proanthocyanidins." *Journal of Agricultural and Food Chemistry* 61, no. 36: 8581–8588. https://doi.org/10.1021/jf402449q.

Tian, H., N. Ling, C. Guo, et al. 2024. "Immunostimulatory Activity of Sea Buckthorn Polysaccharides via TLR2/4-Mediated MAPK and NF-KappaB Signaling Pathways *in Vitro* and *in Vivo*." *International Journal of Biological Macromolecules* 283, no. Pt 2: 137678. https://doi.org/10.1016/j.ijbiomac.2024.137678.

Veberic, R., A. Slatnar, J. Bizjak, F. Stampar, and M. Mikulic-Petkovsek. 2015. "Anthocyanin Composition of Different Wild and Cultivated Berry Species." *LWT—Food Science and Technology* 60, no. 1: 509–517. https://doi.org/10.1016/j.lwt.2014.08.033.

Wang, B., and Y. L. Du. 2013. "Cadmium and Its Neurotoxic Effects." *Oxidative Medicine and Cellular Longevity* 2013, no. 1: 898034. https://doi.org/10.1155/2013/898034.

Wang, R., P. Sang, Y. Guo, et al. 2023. "Cadmium in Food: Source, Distribution and Removal." *Food Chemistry* 405, no. Pt A: 134666. https://doi.org/10.1016/j.foodchem.2022.134666.

Wang, Y., J. Qian, J. Cao, et al. 2017. "Antioxidant Capacity, Anticancer Ability and Flavonoids Composition of 35 Citrus (*Citrus reticulata* Blanco) Varieties." *Molecules* 22, no. 7: 1114. https://doi.org/10.3390/molecules22071114.

Wang, Y., Y. Tang, Z. Li, et al. 2020. "Joint Toxicity of a Multi-Heavy Metal Mixture and Chemoprevention in Sprague Dawley Rats." *International Journal of Environmental Research and Public Health* 17, no. 4: 1451. https://doi.org/10.3390/ijerph17041451.

Wei, F. H., K. Lin, B. J. Ruan, et al. 2024. "Epigallocatechin Gallate Protects MC3T3-E1 Cells From Cadmium-Induced Apoptosis and Dysfunction via Modulating PI3K/AKT/mTOR and Nrf2/HO-1 Pathways." *Peerj* 12: e17488. https://doi.org/10.7717/peerj.17488.

Wu, K. C., J. J. Liu, and C. D. Klaassen. 2012. "Nrf2 activation Prevents Cadmium-Induced Acute Liver Injury." *Toxicology and Applied Pharmacology* 263, no. 1: 14–20. https://doi.org/10.1016/j.taap.2012.05.017.

Yang, D., Y. Ran, X. Li, et al. 2022. "Cyanidin-3-*O*-Glucoside Ameliorates Cadmium Induced Uterine Epithelium Proliferation in Mice." *Journal of Hazardous Materials* 425: 127571. https://doi.org/10.1016/j.jhazmat.2021.127571.

Yu, Z. M., X. M. Wan, M. Xiao, C. Zheng, and X. L. Zhou. 2021. "Puerarin Induces Nrf2 as a Cytoprotective Mechanism to Prevent Cadmium-Induced Autophagy Inhibition and NLRP3 Inflammasome Activation in AML12 Hepatic Cells." *Journal of Inorganic Biochemistry* 217: 111389. https://doi.org/10.1016/j.jinorgbio.2021.111389.

Yuan, B., J. Mao, J. Wang, S. Luo, and B. Luo. 2024. "Naringenin Mitigates Cadmium-Induced Cell Death, Oxidative Stress, Mitochondrial Dysfunction, and Inflammation in KGN Cells by Regulating the Expression of Sirtuin-1." *Drug and Chemical Toxicology* 47, no. 4: 445–456. https://doi.org/10.1080/01480545.2023.2288798.

Zhang, D., Z. P. Yu, W. Z. Zhao, and J. B. Liu. 2022. "Assessment of the Anti-Tumor Activity of Cyanidin-3-*O*-Arabinoside From Apple Against APN, JAK, and EZH2 Target Proteins." *Food Bioscience* 48: 101788. https://doi.org/10.1016/j.fbio.2022.101788.

Zhao, C. J., D. Yu, Z. Q. He, et al. 2021. "Endoplasmic Reticulum Stress-Mediated Autophagy Activation Is Involved in Cadmium-Induced Ferroptosis of Renal Tubular Epithelial Cells." *Free Radical Bio Med* 175: 236–248. https://doi.org/10.1016/j.freeradbiomed.2021.09.008.

Zielinska, A., P. Siudem, K. Paradowska, M. Gralec, S. Kazmierski, and I. Wawer. 2020. "*Aronia Melanocarpa* Fruits as a Rich Dietary Source of Chlorogenic Acids and Anthocyanins: ^{1}H-NMR, HPLC-DAD, and Chemometric Studies." *Molecules* 25, no. 14: 3234. https://doi.org/10.3390/molecules25143234.

Supporting Information

Additional supporting information can be found online in the Supporting Information section.